

A Role for Cytoskeletal Proteins as Modifiers of Mutant Huntingtin
Toxicity

by

Hengameh Zahed Kargaran

DISSERTATION

Submitted in partial satisfaction of the requirements for the degree of

DOCTOR OF PHILOSOPHY

in

Biomedical Sciences

in the

GRADUATE DIVISION

of the

UNIVERSITY OF CALIFORNIA, SAN FRANCISCO

Copyright 2014

by

Hengameh Zahed

Acknowledgements

My PhD experience, like that of many, has been a journey of self discovery as well as a scientific one. I have been truly lucky to benefit from the help of many on this journey.

First and foremost, I dedicate this thesis to my parents, Iran Sabet and Jalil Zahed, who gave up all material possessions, family ties, and social roots to move my siblings and me to the United States so we could pursue the best education and opportunities. Their dreams were large, their bravery unparalleled, and their dedication undeniable. I can never repay them for their sacrifices.

I am also grateful to my parents for giving me two partners in crime to go through life with: my hard-working, brilliant, loving siblings, whose support I have relied so heavily on. My sister, Chakameh Zahed, is a perfect embodiment of a resilient mind meeting the most generous of souls. Thank you for being the older sister I could look up to and for helping me find the will to push through hard times. I learned to not shy away from a challenge watching you boldly become a talented and successful “EECS geek” and excel in a heavily male-dominated field. My brother, Hazhir Zahed, has been the voice of calm and reason throughout my life. I am impressed by your confidence and articulateness and have sought your wisdom time and again. From you I’ve learned that success is the end product of gracefully getting up every time you fall. Your drive and passion in everything you do is inspiring. I am so lucky to have you in my life.

I also want to acknowledge the dedication and support of my best friend, my rock, my love: Erik Ko. None of this would be possible without you. You are the most patient, caring, and understanding human being I have ever met and the best partner I could ask for. From driving me to lab at 3am and sleeping on the couch while I wait for two hours to put the next plate on the microscope, to patiently weathering my ups and downs in lab, you made it possible for me to do this work. Sharing a laugh with you was sometimes the only thing that kept me going during a string of failed experiments. I can never thank you enough for everything you have done and continue to do for me!

Scientifically, I will be forever grateful and indebted to my mentor, Steve Finkbeiner, for taking a chance on me and showing me patience. I have learned so much about the art of being a scientist from you: how to present effectively and memorably, craft a compelling manuscript, approach scientific problems, bring clarity to an idea, and get others excited about our work. Your creativity, dedication to the lab and to science, efficiency, brilliance, and quantitative approach to biology are examples I will aspire to. I am convinced you don't sleep, because there can't be enough hours in a day to accomplish all that you do. I am also grateful for your incredible ability to raise funds. To not have to worry about the cost of doing science during one of the worst funding cycles, when many other labs were struggling to even remain open, is a blessing I can't over-emphasize. I will also always fondly remember your enthusiasm for Halloween and your hospitality, generosity, and masterful culinary skills so elegantly displayed during the yearly feasts at your home.

Science is as much a team sport as an individual pursuit and I am indebted again to Steve for his ability to assemble the perfect team. During my time in the Finkbeiner lab, I was surrounded by an incredibly smart and inspiring group of people and I owe much of my development as a scientist to them. To say it has been a humbling experience is an understatement. The Finkbeiner lab truly has been a second home to me and I have formed so many friendships here that leaving the lab feels like a second migration. Montse Arrasate took me on as a rotation student and taught me everything I needed to know to get started. Working with her was a true joy. I'm not embarrassed to admit that I cried the day she left the lab. In addition to Montse, Gaia Skibinski, Julia Kaye, and Kelly Haston are my role models for being a successful female scientist. They are all forces to be reckoned with: smart, creative, efficient, and thorough, while being truly amazing lab citizens and looking after grad students like me. Gaia (a.k.a "Officer") Skibinski, who I have never seen without a smile on, has been a dear friend to me inside and outside of the lab. We have shared so many coffee chats about lab and life, and I owe you so much. Your friendship and advice mean more than words can explain. Julia Kaye is a free spirit with a contagious passion for science, whom I have admired from the first day I met her. Thank you for always being

willing to listen and to lend a hand with experiments. Kelly Haston has encouraged me to keep going both in the lab and on the running trail and has brightened many days with her humor. I am also fortunate enough to have had Sami Barmada as an exemplary model of a physician-scientist to look up to. I am grateful for the countless hours he let me shadow him in the clinic. Working on his dad jokes long before he even had a kid made for colorful moments. My friendship with Ashkan Javaherian started long before he joined the Finkbeiner lab. He was my first rotation mentor at UCSF in Arnold Kriegstein's lab and I was thrilled when he joined Steve's lab.

Steve has also mentored many graduate students and I have benefitted significantly from overlapping with many of them. Julia Margulis is like a younger but wiser sister to me. We have shared so many happy memories these past years: wine-tasting, celebrating birthdays, singing our hearts out at karaoke, house-boating, sky-diving, exploring Tahoe and Vegas, and many more. Thank you for patiently listening to me during so many lunches and for being one of my closest confidantes. Ian Kratter and Aaron Daub were my MSTP brothers in lab. We joined Steve's lab roughly around the same time, helped each other during the good and bad times, lent a hand for each other's experiments, advised each other, and pushed each other through the program. Ian Kratter: thank you for never letting a moment in lab get dull with your singing, for enriching my life with discussions of science and politics, and for letting me pull pranks on you when we just needed a break. Aaron Daub: you are seriously the nicest human being I have ever met. Inside the lab, we all benefited from your engineering knowledge and mechanical know-how. You kept Robo2 going and answered my middle of the night calls about Robo2 emergencies with the utmost grace. You gave us the Matlab and Pipeline Pilot algorithms that we all used for data analysis. Outside the lab, our hikes, adventures, and dinners together were occasions to look forward to. Mike Ando: part friend, part neighbor, part lab mate, part geek extraordinaire. I will badly miss our "cookie o'clock" discussions of science. You were the technical genius behind Robo3 and our "Master MUG" (Microscope User's Group). I and the rest of the lab owe you so much for your selfless efforts in keeping the microscopes running. Jason Miller (a.k.a Millerpedia or pizza-eating champion of the Finkbeiner lab): we all benefited

from your unapologetic curiosity. There was never a talk you didn't raise your hand at with a thoughtful question, never a paper you hadn't read, never a social or political subject you hadn't thought about. Everything I know about microscopy I learned from him (or from Silvia Foppiano). You challenged us all to think more deeply and understand the methodology we use more thoroughly. Thank you for making me feel like the center of the universe every time we chatted, be it about lab or life, even though you always had so much going on. Eva Ladow was the source of so much knowledge in the lab, the molecular biology and protein chemistry guru we all went to. After Steve, she has been my role model for making beautiful, easily-understandable presentations on complex topics. Thank you for letting me crash on your couch, making us delicious lab-made ice creams and other yummy treats, and teaching me so much. Maya Chandru Overland and Carol Peebles—both witty, wicked smart, and graceful—have always been incredibly generous and open with their advice and their friendship. Erica Korb was a member of the “fun bay,” where we shared many laughs, especially when we proudly made the “stupid trophy” to make ourselves feel better about mistakes we inevitably all made. Thank you for encouraging me to say no when needed.

There are many more brilliant people who I overlapped with in Steve's lab and learned something from every single one of them: Amanda Mason, Adam Ziemann, Andrey Tsvetkov, Matthew Campioni, Lisa Elia, Rebecca Aron, Ana Osoria Oliveria, Jeannette Osterloh, Annie Wang, Kurt Weiberth, Arpana Arjun, Hong Joo Kim, Punita Sharma, Tina Tran, Andre Zandona. There is not enough space in these pages to thank them all the way I should.

Huge thanks also go to my thesis committee members: Robert Edwards and Eric Huang, who also served on my qualifying exam committee. I have greatly benefited from their example, insightful advice and feedback, and thoughtful questions during my committee meetings and on this dissertation.

In addition to my thesis committee members, I had the good fortune of interacting with and learning from several other faculty members at UCSF. Among them are the other members of my qualifying exam

(Anatol Kreitzer and Paul Muchowski) and rotation mentors (Tony Wynshaw-Boris, Bruce Conklin, David Rowitch, and Arnold Kriegstein), all of whom gave generously of their time, resources, and advice.

This work would also not been possible without the work and insight of my collaborators on the tau project. Thank you Eliezer Masliah, Lennart Mucke, Nino Devidze, Iris Lo, and Gui-Qiu Yu.

Several administrators masterfully coordinated schedules and helped me with all the logistical aspects of my training and getting the science done: Kelley Nelson (Finkbeiner lab), Jana Toutolmin and Catherine Norton (Medical Scientist Training program), Lisa Magargal and Monique Piazza (Biomedical Sciences graduate program), and Shirley Freeman (Gladstone)—without your help I'd be lost. Crystal Herron and Gary Howard in the editorial department at Gladstone were incredibly helpful with all writing-related tasks and read every manuscript and proposal quickly and with critical eyes. I also have to thank the three directors of the UCSF MSTP who have kept the program going and supported me throughout my time here so far: Art Weiss, Kevin Shannon, and Mark Anderson.

I owe my scientific journey to several people who encouraged my interests before getting to UCSF and were instrumental in my decision to pursue an MD/PhD training: Ruth Lupu, Miaw-Sheue Tsai, Ella Atlas, Janice Pluth, and Priscilla Cooper. Thank you all for getting me excited about research.

Last, but not least, I would also like to acknowledge my amazing friends outside of lab who have kept me sane and brought dimension to my life: Kelly Quinn, Heather Bennett Schickedanz, Lily Peng, Renatta Knox, and the rest of my MSTP classmates. Your love and support is priceless.

Contributions of Others in Work Presented

The work presented here is the result of the contributions of many.

The following people were significantly involved in the Tau study: Gui-Qiu Yu bred the mice and maintained the study cohort. Iris Lo and Nino Devidze carried out the mouse behavioral studies. Ian Kratter helped with data analysis. Dr. Lennart Mucke was instrumental in the selection of the behavioral tests and has provided insightful feedback on the manuscript. Dr. Eliezer Masliah performed the analysis of neuropathology.

The Actn2 study benefited from the work of the following people: Aaron Daub, Punita Sharma, and Mike Ando developed the robotic microscope systems used for survival analysis. Aaron Daub and Mike Ando also developed the image analysis pipelines. Aaron Daub also helped generate the Htt-N586 constructs. Ian Kratter helped with breeding the mice and RNA extraction. Our collaborators Kai Wang and Hong Li at the Institute for System Biology in Seattle helped with the RNA-Seq analysis.

Abstract

A role for Cytoskeletal Proteins as Modifiers of Mutant Huntingtin Toxicity

By

Hengameh Zahed

Huntington's disease (HD) is an adult-onset monogenic neurodegenerative disorder that can manifest with any combination of motor, cognitive, and psychiatric symptoms. Despite two decades of research since the discovery of the gene, our current understanding of HD pathogenic mechanisms remains incomplete and no disease-modifying therapies exist. A large number of pathogenic mechanisms have been implicated in HD, but the relative importance or order and timing of these processes are still a matter of much debate. Studies in another neurodegenerative disorder, Alzheimer's disease (AD), have shown that deleting the microtubule associated-protein tau reverses cognitive deficits and behavioral abnormalities in multiple AD models, potentially by blocking disease-related synaptic hyper-excitability without affecting normal synaptic transmission. Since excitotoxicity may also contribute to the pathogenesis of HD, we examined whether deleting tau can also prevent abnormalities in a mouse model of HD. Using the BACHD model, we present evidence that deleting tau ameliorates some HD-induced behavioral and neuropathological symptoms. We also explored the extent of transcriptional dysregulation in this mouse model. While we found little evidence for large-scale perturbations in the transcriptional profile of these mice early in their disease progression, we discovered that the actin-bundling protein α -Actinin2 (ACTN2) is down-regulated in BACHD brains. As TAU and ACTN2 are both

cytoskeleton-associated proteins, our work suggests that perturbations in the cytoskeleton may be involved in HD-induced pathogenesis.

Table of Contents

Acknowledgments.....	iii
Contribution of Others in Work Presented.....	viii
Abstract.....	ix
Table of Contents.....	xi
List of Tables.....	xiii
List of Figures.....	xiv
Chapter 1: Introduction to Huntington’s disease.....	1
Chapter 2: Deleting <i>Tau</i> significantly improves behavioral abnormalities and neuropathology in a mouse model of Huntington’s disease	
Abstract.....	8
Introduction.....	9
Methods.....	11
Results.....	16
Discussion.....	21
Chapter 3: Down-regulation of <i>Actn2</i> in the BACHD mouse model of Huntington’s disease	
Introduction.....	40
Methods.....	41

Results.....	48
Discussion.....	52
Chapter 4: Concluding Remarks	67
References.....	69
Publishing Agreement.....	94

List of Tables

Table 1. RNA-Seq read details.	57
Table 2. Striatum-enriched genes commonly dysregulated in HD brains and mouse models are not changed in the BACHD model.	58
Table 3. Summary of gene expression changes between BACHD and WT littermates.	59

List of Figures

Figure 1. Deleting <i>Tau</i> does not significantly alter BACHD-induced motor deficits.	27
Figure 2. Deleting <i>Tau</i> significantly reduces BACHD-induced motor skill learning deficits in the rotarod test.	29
Figure 3. Deleting <i>Tau</i> significantly reduces BACHD-induced deficits in procedural learning in the water T-maze test.	31
Figure 4. Deleting <i>Tau</i> reduces BACHD-induced anxiety-like symptoms.	33
Figure 5. Deleting <i>Tau</i> does not alter body weight in mice.	34
Figure 6. Deleting <i>Tau</i> significantly reduces BACHD-induced striatal and cortical pathology.....	36
Figure 7. Deleting <i>Tau</i> significantly improves the BACHD-induced loss of synaptophysin immunoreactivity.	38
Figure 8. Global correlation of RNA-Seq gene expression counts between BACHD and WT controls suggests few transcriptional changes in the BACHD model.	61
Figure 9. qRT-PCR verification of the expression of selected genes suggested by RNA-seq. ...	62
Figure 10. <i>Actn2</i> mRNA levels are decreased in striata of BACHD mice.	63
Figure 11. ACTN2 protein levels are reduced in striata of BACHD mice.	64
Figure 12. ACTN2 protein is highly expressed in striatal neurons.	65

Figure 13. ACTN2 over-expression shows an epistatic interaction with mHtt-dependent toxicity.....66

Chapter 1: Introduction to Huntington's disease

Poly-glutamine Disorders

Huntington's disease (HD) is a rare but devastating and fatal neurodegenerative disorder that manifests most often in adulthood as any combination of abnormal motor movements, psychiatric changes, and cognitive deficits (Roze et al., 2008). It occurs when the normally variable number of CAG tri-nucleotide repeats in the first exon of the *IT-15* gene expands beyond a critical minimal threshold of 36-40, leading to the expansion of the poly-glutamine (polyQ) stretch in the N-terminus of its widely expressed product, huntingtin (HTT) (The Huntington's Disease Collaborative Research Group, 1993). There is an inverse relationship between the length of the polyQ stretch and the disease onset. However, among the most common HD alleles (40-50 repeats), only roughly 50% of the variability in the age of onset is explained by the length of the polyQ stretch, implying that the remainder is influenced by modifiers, be they genetic and/or environmental (Wexler, 2004).

Similar expansions in eight other genes also lead to neurodegenerative disorders. Expanded polyQ stretches may have intrinsic neuronal cytotoxicity (Lipinski and Yuan, 2004; Perutz and Windle, 2001; Ross, 1995). However, this mechanism alone does not explain how polyQ expansions in each of the disease-associated proteins cause the degeneration of different, though sometimes overlapping, circuits of neurons. Furthermore, a tissue-specific pattern of degeneration occurs in each disease, even though the polyQ containing proteins such as mutant HTT (mHTT) are often expressed widely in the brain and other tissues (Ide et al., 1995; Li et al., 1993; Strong et al., 1993). For example, in HD a striking atrophy of the striatum and also the

cortex can be seen. These features suggest that the protein context of the polyQ-containing protein is crucial to the manifestation of symptoms in each of these disorders.

PolyQ diseases are considered protein conformation disorders in which the mutant protein adopts aberrant conformation(s) (Kuhn et al., 2007; Ross, 1995; Van Raamsdonk et al., 2006). Inclusion bodies (IBs) have been identified in human diseased brains in HD and other polyQ disorders. Both cytoplasmic and nuclear inclusions appear to mark the pathology of polyQ disorders, but inclusions themselves have been shown to not be causative in the disease process and may instead be a coping mechanism via sequestering one or more diffuse toxic species (Arrasate et al., 2004a; Slow et al., 2005; Miller et al., 2010).

Proposed functions of wild-type Huntingtin

HTT is a large, widely expressed, 347 kDa protein that localizes predominantly to the cytoplasm. At the level of the organism, HTT has an essential role in embryonic development and its absence leads to embryonic lethality (Duyao et al., 1995; Nasir et al., 1995; Zeitlin et al., 1995). Furthermore, HTT may also be important in the postnatal brain, as its inactivation in mice during adulthood leads to reduced life span, neuropathology, and motor deficits (Dragatsis et al., 2000).

What exactly wild-type HTT does in the cell to prevent the above phenotypes remains elusive. Because of its large size, HTT has not been amenable to detailed structural studies of the full-length protein. Additionally, the HTT protein bears little homology to other known proteins (Harjes and Wanker, 2003). Nonetheless, HTT appears to contain 16 putative HEAT repeats arranged in four main clusters downstream of the polyQ stretch (Tartari et al., 2008). These domains are sequences of approximately 40-50 amino acids that occur multiple times within a

protein and are important for formation of protein-protein interactions (Andrade et al., 2001). Accordingly, HTT has been proposed to act as a protein scaffold and major protein interaction hub. Indeed, searches for HTT-interacting proteins have revealed more than 700 interaction partners (Kaltenbach et al., 2007; Shirasaki et al., 2012). Interestingly, HTT-interacting proteins include several cytoskeletal proteins, such as the HTT-interacting protein 1 (HIP1), tubulin, dynactin, ubiquitin conjugating enzyme E2-25K, Src homology region 3-containing Grb2-like protein 3 (SH3GL3), HTT-associated protein 1 (HAP1), postsynaptic density-95 (PSD95), the cytoskeletal ras-related protein Duo, and SlaI, a cytoskeletal assembly protein involved in the nucleation of actin microfilaments. These proteins play roles in clathrin-mediated endocytosis, vesicle transport, cell signaling, morphogenesis, and transcriptional regulation, suggesting that HTT may also be involved in these processes (Harjes and Wanker, 2003).

Pathogenic mechanisms in HD

Despite two decades of research since the discovery of the gene, our current understanding of the molecular mechanisms by which the polyQ expansion in HTT causes selective neurodegeneration remains incomplete. Both gain-of-function of the mutant protein and loss-of-function of the normal protein have been described in HD (Schulte and Littleton, 2011). A large number of pathogenic mechanisms have been implicated in HD, including conformational changes in the mutant protein that alter some of the many interactions of wild-type HTT and induce new abnormal ones (Li and Li, 2004), proteolysis of mHTT to generate toxic fragments, transcriptional dysregulation, impairment of the proteasome, mitochondrial dysfunction and energetic deficits, *N*-methyl-D-aspartate receptor (NMDAR)-mediated Ca²⁺ dyshomeostasis and

excitotoxicity, and deficits in vesicular trafficking and axonal transport (Gil and Rego, 2008; Finkbeiner, 2011). These mechanisms need not be mutually exclusive. Nonetheless, the exact nature of these processes, their relative importance, their order, and their timing with respect to the development of symptoms are still a matter of much debate. This dissertation focuses on two of these mechanisms: excitotoxicity and transcriptional dysfunction.

Excitotoxicity in HD

Excitotoxicity was among the first mechanisms implicated in HD pathogenesis. Even before the discovery of the Htt gene, systemic injection of excitotoxic glutamate analogs (such as quinolinic acid) was shown to produce selective pathology in the striatum, which receives extensive excitatory glutamatergic inputs from the cortex, in a pattern mimicking HD pathology (Beal et al., 1986; McGeer and McGeer, 1976). While these early observations have since been disputed, they sparked further investigations into the contribution of excitotoxicity in HD, the results of which have implicated both pre- and post-synaptic mechanisms of excitotoxicity in the disease.

Expression of mhtt appears to sensitize neurons to excitotoxins or repeated glutamatergic stimulation of NMDARs, at least in the early stages of disease progression (Levine et al., 1999; Zeron et al., 2002; Tang et al., 2005; Zhang et al., 2008). This sensitization may be due to hypersensitivity of post-synaptic NMDARs on striatal projection neurons, mediated by alterations in the subunit composition, post-translational modification, trafficking, and function of glutamate receptors (Chen et al., 1999; Levine et al., 1999; Sun et al., 2001; Li et al., 2003; Metzler et al., 2007; Heng et al., 2009), and/or altered signaling downstream of these receptors. Other studies have also provided evidence for pre-synaptic mechanisms for excitotoxicity in HD. These include increased generation of the endogenous NMDAR agonist quinolinic acid and its

precursor 3-hydroxykynurenine (Guidetti et al., 2006; Campesan et al., 2011), increased glutamate release and excitatory output from cortical afferents (André et al., 2011), reduced inhibition onto cortical pyramidal cells (Spampanato et al., 2008), and impaired clearance of glutamate from the synaptic cleft by glia (Liévens et al., 2001; Hassel et al., 2008; Miller et al., 2008). In the later stages of the disease, adaptive responses to excitotoxicity may ultimately lead to a progressive loss of connectivity between the cortex and striatum, contributing to the progression of the disease phenotypes.

Despite the above evidence, HD clinical trials that inhibit the NMDAR or glutamate release to block excitotoxicity have shown mixed results in HD animal models and mostly failed to show benefits in HD patients (Kremer et al., 1999; Landwehrmeyer et al., 2007) and some carefully controlled animal studies (Tallaksen-Greene et al., 2010), casting doubt on the role of excitotoxicity in HD.

Still, excitotoxicity may be a common mechanism in a variety of neurodegenerative diseases (Aarts and Tymianski, 2003), and approaches to target this mechanism in the context of one disease may be beneficial to others as well. For example, recent studies have suggested that hyper-excitability also plays an important role in Alzheimer's disease (AD) and that deleting the *Tau* gene reverses hyper-excitability and normalizes cognitive deficits of AD mice (Ittner et al., 2010; Roberson et al., 2007, 2011). There is little evidence that connects TAU to HD. However, because deleting *Tau* improves hyper-excitability and cognitive deficits in one dementing disorder, we hypothesized that it might mitigate analogous deficits in HD mouse models. In chapter 2, we report the results of our studies testing this hypothesis using the bacterial artificial chromosome HD (BACHD) mouse model, which expresses full-length human HTT with 97

consecutive glutamines and recapitulates the behavioral phenotypes and neurodegeneration seen in HD (Gray et al., 2008).

Transcriptional dysfunction in HD

A large number of studies examining gene expression patterns in HD have been performed. These studies have revealed transcriptional changes in HD patients (Hodges et al., 2006) and several HD mouse models (Chan et al., 2002; Desplats et al., 2006; Kuhn et al., 2007; Mazarei et al., 2009; Becanovic et al., 2010; Thomas et al., 2011), in isolated mHTT-expressing cells in culture (Sipione et al., 2002; Runne et al., 2008), and in human neural stem cells derived from induced pluripotent stem cells of HD patients (The HD iPSC Consortium, 2012). Interestingly, extent of transcriptional dysregulation correlates with the degree of tissue involvement in the disease (Hodges et al., 2006), with the largest changes observed in the striatum. The array of genes altered at the RNA level in HD is diverse and includes genes important for neuronal function such as neurotransmitter receptors, intracellular signaling molecules and second messengers, cytoskeletal proteins, and synaptic organization and release proteins. Therefore, transcriptional dysfunction is hypothesized to play a major role in HD (Cha, 2000; Sugars and Rubinsztein, 2003; Seredenina and Luthi-Carter, 2012).

The mechanistic basis of these changes is an active area of research. Mutant HTT may have a direct effect on RNA biogenesis. Supporting this, aberrant interactions between mHTT and transcriptional regulatory proteins such as TATA box binding protein (TBP), the TFIID subunit TAFII-130, Sp1, NCoR, CtBP, CA150, and REST/NRSF (Harjes and Wanker, 2003), have been described. Some of these aberrant interactions, especially the one with REST/NRSF which leads to repression of neuronal selective genes, may contribute to the selective vulnerability of neurons

in HD. Furthermore, some studies have suggested a role for mHTT in disrupting the activity of histone acetyl transferases that act as chromatin remodeling enzymes, and correction of transcriptional dysregulation by preventing histone deacetylation (HDAC inhibitors) has been shown to ameliorate mHTT toxicity in flies and mice (Steffan et al., 2001; Jia et al., 2012). Nonetheless, some transcriptional changes may also stem from neurodegenerative changes to tissue architecture and composition. The study by Hodges and colleagues (Hodges et al., 2006) suggests that gene expression changes are not strictly the result of cell loss or changes in tissue architecture. However, studies in the YAC models—that express full-length mHTT and show behavioral deficits, but lack prominent neurodegeneration as a feature until late in the disease—have identified fewer transcriptional changes, suggesting that large-scale perturbations in mRNA levels are not directly a result of mHTT expression and are not required for the development of the neurologic phenotypes observed in these models (Chan et al., 2002).

Regardless of the exact mechanism behind transcriptional changes in HD, the functional significance of these changes remains largely unknown, as the change in transcript level for any given gene may be etiologic and mediate toxic effects, a correlative epiphenomenon, or an adaptive homeostatic response by the cell or organism to the disease insult.

As discussed earlier, the BACHD model is commonly used to study disease mechanisms and therapeutic strategies in HD. However, the presence and degree of transcriptional dysfunction in this model has not been explored. In chapter 3, we summarize the results of our studies on the role of transcriptional dysfunction in this model. Importantly, this model, similar to the YACHD model, does not have a significant neurodegenerative phenotype until late in the course of the disease (Gray et al., 2008), allowing us to determine the extent of transcriptional dysfunction in the absence of overt neuropathology.

Chapter 2: Deleting *Tau* significantly improves behavioral abnormalities and neuropathology in a mouse model of Huntington's disease

Abstract

Huntington's disease (HD) is an adult-onset monogenic neurodegenerative disorder that can manifest with any combination of motor, cognitive, and psychiatric symptoms. The cause of dementia in HD is not known and no therapies exist. Studies in another neurodegenerative dementing disorder, Alzheimer's disease (AD), have shown that deleting the microtubule associated-protein *Tau* reverses cognitive deficits and behavioral abnormalities in multiple AD models, potentially by blocking disease-related synaptic hyperexcitability without affecting normal synaptic transmission. Since excitotoxicity may also contribute to the pathogenesis of HD, we examined whether deleting *Tau* can also prevent abnormalities in a mouse model of HD. Using the BACHD model, we show that deleting *Tau* ameliorates the cognitive and psychiatric-like symptoms induced by mutant HTT (mHTT) without altering motor deficits. Furthermore, we show that deleting *Tau* robustly protects against mHTT-induced striatal and cortical atrophy and synapse loss. These data suggest that TAU plays a novel permissive role in HD pathology. Thus, currently developing therapies aimed at reducing TAU for the treatment of AD may also be useful for treating cognitive and psychiatric symptoms and ameliorating neurodegeneration in HD patients.

Introduction

Huntington's disease (HD) is a dominantly inherited neurodegenerative disorder that primarily affects the corticostriatal circuit (Cepeda et al., 2007), and is caused by the expansion of the CAG repeats in the *HTT* gene (The Huntington's Disease Collaborative Research Group, 1993). While HD is classified as a movement disorder due to the involuntary choreic movements often present, it can also cause psychiatric symptoms and dementia, which can equally disrupt the lives of HD patients (Finkbeiner, 2011). Unfortunately, the cause of dementia in HD is unknown and novel therapies for the treatment of dementia related to HD are needed.

Previous studies found that the cortex may become hyper-excitabile early in HD. Loss of inhibition onto cortical pyramidal cells (Spampanato et al., 2008) and increased excitatory output from the cortex (André et al., 2011) have been reported in HD mouse models. Additionally, systemic injection of excitotoxins produce selective pathology in the striatum (a key synaptic target of the cortex), which mimics HD pathology (Beal et al., 1986; McGeer and McGeer, 1976). Furthermore, the composition, function, and trafficking of glutamate receptors is altered in HD (Chen et al., 1999; Levine et al., 1999; Li et al., 2003; Metzler et al., 2007; Heng et al., 2009). Finally, the aggressive juvenile form of HD can present with epileptic seizures (Cloud et al., 2012). However, HD clinical trials that inhibit the *N*-methyl-D-aspartate receptor (NMDAR) or glutamate release to block excitotoxicity have failed to show benefits (Kremer et al., 1999; Landwehrmeyer et al., 2007), casting doubt on the role of excitotoxicity in HD.

Recent studies have demonstrated an important role for hyper-excitability in another dementing disorder, Alzheimer's disease (AD). As in HD, overt seizures are rare in AD. However, AD animal models and patients show significant cortical hyper-excitability and adaptive tissue

changes seen in epilepsy (Palop et al., 2011, 2007; Verret et al., 2012). Importantly, certain antiepileptic medicines reverse changes in behavior and histology in AD mice (Sanchez et al., 2012), indicating that hyper-excitability may be pathogenic. Deleting the *Tau* gene also reverses hyper-excitability and normalizes cognitive deficits of AD mice (Ittner et al., 2010; Roberson et al., 2007, 2011). In these studies, deleting *Tau* also prevents drug-induced seizures in normal mice, suggesting that deleting *Tau* might correct cognitive deficits in AD model mice by blocking disease-related synaptic hyper-excitability without affecting normal synaptic transmission. Since *TAU* mutations also cause another dementing disorder, frontotemporal dementia (Spillantini and Goedert, 2013), *TAU* may broadly contribute to symptoms of dementia in neurodegenerative diseases.

The microtubule-associated protein *TAU* was initially identified in the 1970s as a microtubule-assembly factor. However, recent studies have uncovered additional roles for *TAU* in cytoskeletal organization and modulation of signaling pathways through scaffolding. *TAU* inclusions occur in a variety of neurodegenerative disorders such as AD, cortico-basilar degeneration, chronic traumatic encephalopathy, frontotemporal lobar degeneration with *TAU* inclusions (FTLD-*TAU*), and others that are collectively referred to as tauopathies (Morris et al., 2011b).

Though there is little evidence that connects *TAU* to HD, we hypothesized that deleting *Tau* might normalize cognitive deficits in HD mouse models. If deletion of *Tau* is protective in HD, it could expand the indications for anti-tau therapies and create additional options for the clinical development of such therapeutics since clinical trials for HD are generally believed to be easier and more sensitive than those for AD. Moreover, a number of pharmaceutical companies are actively developing anti-tau therapies for AD. To evaluate this, we used the bacterial artificial

chromosome HD (BACHD) mouse model, which expresses full-length human HTT with 97 consecutive glutamines and recapitulates the behavioral phenotypes and neurodegeneration seen in HD (Gray et al., 2008). We show that deleting *Tau* ameliorates the cognitive and psychiatric-like symptoms induced by mutant HTT without altering motor deficits and robustly protects against neuropathology.

Materials and Methods

Mouse Models

BACHD mice on an FVB background (Gray et al., 2008) were crossed with *Tau*^{-/-} mice (Dawson et al., 2001) on a C57BL/6 background. Mice were group housed with a normal light–dark cycle in a clean facility and *ad libitum* access to food and water. Age-matched progeny were used for behavioral testing. For all analyses, the experimenter was blinded to the genotype of the mice. Both male and female mice were included, and since no differences were observed between the sexes, results were pooled. All experiments were approved by the Committee on Animal Research of the University of California, San Francisco (Approval Number AN087648-03B).

Behavioral Tests

For all behavioral tests, mice were given at least 30 min to acclimate to the room prior to testing. The testing apparatus was cleaned with 70% ethanol between tests.

Open field. A Flex-Field/Open Field Photobeam Activity System (San Diego Instruments, San Diego, CA) was used to detect spontaneous horizontal and vertical movements in mice and assess their locomotor activity. Each mouse was placed in the center of a clear plastic chamber

(41×41×30 cm) consisting of two 16×16 photobeam arrays and given 15 min to explore under normal light. Beam breaks were recorded as movement and when recorded on the higher of the two arrays, was classified as rearing.

Rotarod. Mice were simultaneously tested, five at a time, on the Rota-Rod (Med Associates Inc, St. Albans, VT) under normal light. A computer recorded photobeam interruptions when mice fell off the rod. Photobeams were also interrupted by the tester if the mouse held onto the rod without walking for three full rotations. Mice were first trained on the Rota-Rod with three trials at a constant speed of 16 rpm and inter-trial interval of 15 minutes. On the second and third day, mice were tested in an accelerating rotarod paradigm (4 rpm to 40 rpm, increasing 4 rpm every 30 s). Three morning and three afternoon trials each lasted 5 min. The inter-trial resting period was at least 15 min and the morning and afternoon sessions were 2 h apart. Latency to fall for each mouse was recorded.

Balance beam. The balance beam test consisted of two platforms, one of which contained an opaque box, connected by a removable plastic beam. The first day of training consisted of two guided trials (mice placed on a thick round beam a few inches from the box and led into the box), followed by three unguided trials across the whole length of the beam with a maximum of 60 s per trial and approximately 10 min between trials. The unguided trials were repeated on the second day. On the third day, the thick beam was replaced with a thin square beam and the mice were tested three times. Videotaped trials were analyzed for average latency to cross the thin beam and the average number of foot slips during the testing sessions. A trial was excluded from analysis if the mouse dragged its hind limbs across the beam for >50% of the distance.

Water T-maze. Mice were singly housed and acclimated to the testing room two days before testing. A curtain prevented the mice from seeing extra-maze cues placed around the room. On

day 1, mice were given two 90 s pre-training trials to swim down a rectangular channel, find a platform hidden 1.5 cm below the water surface, and remain there for 5 s before being removed. Drop location was alternated between trials. During each day of the next phase (days 2–5), mice were placed at the base of the water T-maze and given three 60 s trials at least 5 min apart to find the hidden escape platform under red light. The platform remained in the same location for each mouse, but was counterbalanced on either the left or right side for different mice. In the reversal phase (days 6–10), the hidden escape platform was located on the opposite side of the original training location in days 2–5. In all phases, any mouse that did not reach the platform was guided to the platform where it had to remain for 5 s before being returned to its home cage. Distance traveled and latency to reach platform, average swim speed, and errors (defined as the mouse entering the incorrect arm before entering the correct one) were recorded.

Elevated plus maze. The elevated plus maze (EPM) consisted of four elevated runways (63 cm above the ground): two open arms (without walls) and two closed arms (with walls) (Hamilton-Kinder, Poway, CA). Mice were placed at the junction between the open and closed arms and allowed to explore for 10 min. Total distance traveled and time spent in open and closed arms were calculated based on infrared photo-beam breaks. General locomotor activity was measured by total distance traveled and total number of crosses into either open or closed arms. Anxiety-like behaviors were assessed by measuring the percentage of time spent in, or of crosses into, the open arms. Distance traveled in the open arms was used to determine if mice were freely moving or freezing due to fear.

Novelty-suppressed feeding. Testing was performed in the dark with the testing box illuminated. Mice were fasted for 24 h before testing, then placed in the corner of the brightly lit arena with a food pellet in the center and were allowed a maximum of 5 min in the test box. The latency to

reach the food and start feeding was used as a measure for depressive-like behavior. Mice were then removed, immediately placed in their home cage, and allowed to eat for 5 min uninterrupted. Post-test food consumption was measured as a control for potential feeding differences.

Stereology and Immunohistochemistry

In accordance with NIH guidelines for the humane treatment of animals, mice were deeply anesthetized with Avertin and flush-perfused transcardially with 0.9% saline. Brains were divided sagittally. The right hemisphere was flash frozen in liquid nitrogen, while the left hemisphere was post-fixed in phosphate-buffered 4% paraformaldehyde (pH 7.4) at 4°C for 48 h and serially sectioned at 40 µm with a Vibratome 2000 (Leica, Germany). An experimenter blinded to genotype analyzed all brain sections. We utilized the Cavalieri method for volume analysis (Everall et al., 1997; Sonmez et al., 2010). Briefly, the region of interest (neocortex) in each cresyl violet-stained section was selected with a 4x objective on an Olympus BX51 microscope (Olympus, Denmark). Each region was then divided into randomly selected squares by Stereo-Investigator software (MBF bioscience, Williston, VT). An average of 25 squares/area in each section was analyzed. The striatal volume was determined in serial sections stained with cresyl violet by point counting and Cavalieri's rule. Volume was computed and corrected for shrinkage (Rosen and Williams, 2001).

The number of neurons immunoreactive to NeuN antibody (mouse monoclonal; Millipore, Billerica, MA) was estimated utilizing unbiased stereological methods (Jaffar et al., 2001). Hemi-sections containing the neocortex and striatum were outlined using an Olympus BX51 microscope running StereoInvestigator 8.21.1 software (Micro-BrightField, Cochester, VT). Grid

sizes for the striatum and neocortex were 900×900 and 300×300 μm, respectively, and the counting frames were 40×40, and 50×50 μm, respectively. The average coefficient of error for each region was 0.9. Sections were analyzed using a 100×1.4 PlanApo oil-immersion objective. A 5-μm high dissector allowed for 2-μm top and bottom guard-zones.

For analysis of synapses, serial sections were immunostained with anti-synaptophysin antibody (mouse monoclonal, clone SY38; Millipore, Billerica, MA), as previously described (Kwan et al., 2012), and analyzed at 63x with the Olympus BX51 microscope.

Statistical Analysis

Data were analyzed using Prism (GraphPad Software, La Jolla, CA). Most measures were analyzed by two-way ANOVA followed by Sidak's post-hoc test with selected comparisons, unless otherwise noted. Only influential data points—defined as greater than two standard deviations (SD) from the mean for their group whose inclusion vs. omission significantly altered the results of the statistical analysis—were excluded from analysis. In data where the variance between groups was severely unequal (Bartlett's test $p < 0.0001$), the data were transformed by either a square-root or log transformation to normalize variance between the groups. The transformation that best normalized variance was then analyzed by two-way ANOVA and a Sidak's post-hoc test. Because of the lack of normal distribution of the data from the novelty-suppressed feeding test, Kaplan–Meier survival analysis was used (Samuels and Hen, 2011). Animals that did not eat during the 5 min testing period were censored. Gehan-Breslow-Wilcoxon test was used to evaluate differences between experimental groups.

Results

To evaluate the effects of deleting *Tau* on mHTT-mediated pathology *in vivo*, we first crossed *Tau* knockout (*Tau*-ko; a.k.a. *Tau*^{-/-}) mice with BACHD mice that express mHTT to generate BACHD/*Tau*^{+/-} F1 progeny. These were then crossed with *Tau*^{+/-} mice. Offspring of all genotypes, including the BACHD/*Tau*-ko mice, appeared healthy at birth, were viable, and did not exhibit any gross deficits at a young age, suggesting that the combination of deleting *Tau* and expressing mHTT does not have a deleterious effect on mouse development. We then examined the mice for motor, cognitive, and psychiatric deficits that are a hallmark of HD at nine months of age, when BACHD mice were shown to exhibit robust HD-like deficits (Gray et al., 2008; Pouladi et al., 2012).

Deleting *Tau* does not affect mHTT-induced motor deficits

The most-studied clinical feature of HD, in both humans and animal models, is late-onset motor deficits. To assess the effect of deleting *Tau* on the development of HD-like motor deficits, we used three separate paradigms that measure varying and overlapping aspects of motor function. First, we assessed the spontaneous general activity, motor function, and exploration in the open-field (Brooks and Dunnett, 2009). Second, we compared the baseline motor coordination and posturing ability of mice during the first trial of a fixed-speed rotarod test, which is the most commonly used test of motor function in rodent models of HD (Pouladi et al., 2013). Third, we used the balance beam test, another commonly used test of motor coordination, (Brooks and Dunnett, 2009). As expected, BACHD mice showed reduced ambulatory activity in the open-field (Fig. 1A), decreased latency to fall in the rotarod (Fig. 1B), and increased slips in the balance beam (Fig. 1C) when compared to their wild-type (WT) littermates. Deleting *Tau*,

regardless of BACHD status, did not significantly affect any of these measures (Fig. 1). These data suggest that deleting *Tau* does not modify the baseline hypo-activity and motor-coordination deficits induced by mHTT expression in BACHD mice.

Deleting *Tau* reduces mHTT-induced cognitive deficits

In addition to deficits in motor performance, HD can cause cognitive abnormalities such as impair executive functions and delay acquisition of new motor skills (Walker, 2007). We assessed the effect of deleting *Tau* on striatal-dependent motor skill learning by examining performance of mice across in repeated trials of the rotarod test. During three initial trials at a fixed-speed (16 rpm), WT and *Tau*-ko mice showed robust motor learning, with a nearly two-fold increase in their average latency to fall (Fig. 2A). In contrast, BACHD mice failed to improve over those three trials. BACHD/*Tau*-ko mice, however, showed improvement by the third trial (Fig. 2A). Mice were then switched to the accelerating rotarod paradigm where the rotation speed increased from 4 to 40 rpm at a rate of 4 rpm every 30 seconds. Here, WT and *Tau*-ko mice were already performing near their maximal capacity, so they did not significantly improve in further trials of the accelerating rotarod (Fig. 2B). In contrast, BACHD and BACHD/*Tau*-ko mice began with a significantly lower latency to fall than controls. With further training, both BACHD and BACHD/*Tau*-ko mice improved their latency to fall. However, BACHD/*Tau*-ko mice learned the task faster and outperformed BACHD mice on most trials (Fig. 2B). Since we did not observe baseline improvements in motor performance by deleting *Tau* (Fig. 1), we believe that the enhanced performance of the BACHD/*Tau*-ko mice after repeated trials of the rotarod is likely not due to effects on motor function. These data demonstrate that deleting *Tau* improves the deficit of BACHD mice in motor skill learning.

Next, we sought to determine if deleting *Tau* modifies mHTT-induced deficits in striatal-dependent procedural learning. For this, we used the water T-maze test in which mice are given a simple, two-choice learning test that is egocentric and striatal-dependent (Van Raamsdonk et al., 2005b). First, we analyzed the average latency of the different genotypes to reach the platform. Compared to WT littermates, BACHD mice showed a greater latency to reach the platform on most days of training (Fig. 3A). To understand whether these differences resulted from a motor or cognitive deficit, we examined the frequency of errant trials and individual swim times. We quantified errant trials by assigning mice a score of 1 if they turned into the correct arm and 0 if they first turned into the incorrect arm. Initially, mice of all genotypes entered the correct arm at chance. By the third and fourth day of training (trials 7–12), however, all WT and *Tau*-ko mice learned to turn into the correct arm (Fig. 3B; WT: 0 of 60 incorrect trials; *Tau*-ko: 0 of 48 incorrect trials). In contrast, BACHD mice still entered the incorrect arm in a small number of trials (BACHD: 9 of 138 incorrect trials), indicating that mHTT expression causes mild cognitive deficits. BACHD mice lacking *tau*, however, made significantly fewer errors (BACHD/*Tau*-ko: 1 of 102 incorrect trials vs. 9 of 138 for BACHD mice; Fisher's exact test $p = 0.047$), suggesting that deleting *Tau* ameliorates cognitive deficits in BACHD mice. Analysis of swim speeds across trials revealed that BACHD mice swim significantly slower than their WT and *Tau*-ko littermates (Fig. 3C). While a slower swim speed may partially contribute to the increased latency of BACHD mice to reach the platform compared to controls, deleting *Tau* did not affect the swim speed of BACHD mice. These data suggest that deleting *Tau* ameliorates the cognitive deficits we observed in BACHD mice in the water T-maze.

Deleting *Tau* ameliorates mHTT-induced affective deficits

The third domain of HD-induced symptoms includes psychiatric disturbances such as depression, anxiety, and altered mood (Paulsen et al., 2001). To test for anxiety and depressive-like behaviors, we used two different paradigms. First, we used the elevated plus maze (EPM) to measure rodent anxiety (Carola et al., 2002). Unlike other reports (Lundh et al., 2012, 2013), we observed no differences among the genotypes in any of the parameters measured in the EPM (data not shown). Second, we tested mice in the novelty-suppressed feeding paradigm, which measures the latency of fasting-motivated animals to eat in an aversive environment and is sensitive to the use of both anxiolytics and chronic antidepressants (Samuels and Hen, 2011). In this test, BACHD mice showed greater latency to eat than WT (Fig. 4A; median latency for WT = 6.00s and for BACHD = 48.50s; 95% CI of BACHD to WT ratio = 3.681–17.75). To ensure that this difference is not due to changes in appetite, we compared food consumption after mice were returned to their home cage and found similar levels between the two groups (Fig. 4B). We then asked whether deleting *Tau* affects the increased latency of BACHD mice to eat in a novel environment. BACHD/*Tau*-ko mice and their *Tau*-ko littermates had similar latencies to eat (Fig. 4A; median latency for *Tau*-ko = 25.0 s and for BACHD/*Tau*-ko = 22.00 s; 95% CI of BACHD/*Tau*-ko to *Tau*-ko ratio = 0.3953–1.959), which were significantly shorter than that of the BACHD mice. Again, *Tau*-ko and BACHD/*Tau*-ko mice ate similar amounts of food upon returning to their home cage. These results suggest that deleting *Tau* may also ameliorate depressive-like symptoms in BACHD mice.

Deleting *Tau* does not alter weight gain in BACHD mice

The increased body weight of transgenic mice expressing full-length mHTT, such as BACHD and YACHD mice (Gray et al., 2008). To determine if the improved behavior upon deletion of *Tau* is influenced by changes in weight, we compared the weight of mice at the time of

behavioral testing. As expected, BACHD mice weighed significantly more than WT. However, deleting *Tau* did not affect weight gain (Fig. 5). Furthermore, correlation analyses did not show a relationship between weight and performance in any of the behavioral paradigms tested in this study (data not shown). Therefore, changes in weight are not responsible for the rescued behavioral deficits observed when *Tau* is deleted in BACHD mice.

TAU mediates mHTT-induced neuropathology

To assess the effect of deleting *Tau* on mHTT-induced neuropathology, we analyzed the brains of mice that had undergone behavioral testing at 14 months. We first focused our analysis on the striatum, the earliest and most affected area of the brain in HD (Vonsattel and DiFiglia, 1998). Consistent with previous studies (Gray et al., 2008), we found that BACHD mice have a significantly reduced striatal volume (Fig. 6A). Deleting *Tau* alone did not affect striatal volume, but did reverse the mHTT-induced loss in striatal volume in BACHD mice (Fig. 6A). Furthermore, striatal neuron count, determined by staining for the neuronal nuclear antigen NeuN, was also significantly lower in BACHD mice than WT controls, indicating mHTT-induced neurodegeneration (Fig. 6B). In contrast, the striatal neuron count in BACHD/*Tau*-ko mice was higher and statistically indistinguishable from their WT littermates and *Tau*-ko mice (Fig. 6B). The increase in striatal neuron count in BACHD/*Tau*-ko mice compared with BACHDs approached, but did not achieve the 0.05 criterion. Together, these data demonstrate that deleting *Tau* has a protective effect on mHTT-induced striatal pathology.

In addition to the striatum, neuropathological changes are also observed in the cortex of HD patients and animal models (Vonsattel and DiFiglia, 1998; Rosas et al., 2002; Gray et al., 2008). In our study, BACHD mice had significantly reduced cortical volumes (Fig. 6C) and NeuN

counts (Fig. 6D) than WT mice. Deleting *Tau* in BACHD mice resulted in an intermediate phenotype that was not significantly different from either BACHD or *Tau*-ko littermates (Fig. 6C), suggesting that deleting *Tau* partially improves cortical volume. Additionally, deleting *Tau* completely reversed the BACHD-induced decrease in cortical NeuN counts (Fig. 5D), but did not affect cortical measures on its own. These findings suggest that deleting *Tau* also improves cortical deficits caused by mHTT expression.

As a separate measure of neuropathology, we also quantified levels of the pre-synaptic marker synaptophysin in striatal and cortical areas. Similar to previous studies (Bouchard et al., 2012; Kwan et al., 2012), we observed significantly lower synaptophysin levels in both brain regions of BACHD mice relative to WT littermates (Fig. 7). Deleting *Tau* significantly improved the synaptophysin levels of BACHD mice, without affecting synaptophysin levels in the absence of mHTT. These results provide further support that TAU plays an important role in mHTT-induced neuropathology.

Discussion

By genetically knocking out *Tau* in BACHD mice, we discovered that TAU is an important regulator of mHTT-induced behavioral deficits. Specifically, we show that deleting *Tau* improves cognitive deficits, such as motor (Fig. 2) and procedural learning (Fig. 3), and anxiety-like phenotypes (Fig 4). In contrast, deleting *Tau* neither improves nor worsens the baseline hypo-activity or motor and coordination deficits in BACHD mice (Fig. 1). Importantly, the behavioral phenotypes of BACHD mice in our study are comparable to previous studies of these mice (Gray et al., 2008; Menalled et al., 2009; Pouladi et al., 2012; Abada et al., 2013).

Furthermore, our observations that *Tau*-ko mice perform as well as control littermates in all tests agrees with previous reports in which deleting *Tau* was generally well tolerated (Roberson et al., 2007; Ittner et al., 2010; Morris et al., 2011a).

We also found that deleting *Tau* ameliorates mHTT-induced neuropathology in BACHD mice. Similar to a report of 12-month-old BACHDs (Gray et al., 2008), we show that 14-month-old BACHD mice exhibit cortical and striatal volume loss (Fig. 6), which may result from loss of NeuN+ neurons (Fig. 6) and synapses (Fig. 7) in these areas. We are the first to report a loss of neurons in the BACHD model. While Gray and colleagues (2008) observed dark degenerating neurons in the striata of 12-month-old BACHD mice, they did not see a difference in the number of NeuN+ neurons, suggesting that striatal neurons are degenerating at 12 months of age, but have not yet been lost. Thus, we speculate that the loss of neurons in this model occurs between 12 and 14 months of age. Our finding of synapse loss, as determined by reduced synaptophysin immunostaining, in BACHD mice is in agreement with previous observations (Bouchard et al., 2012; Kwan et al., 2012; Shirendeb et al., 2012) and mimics deficits seen in HD patients (Goto and Hirano, 1990). Remarkably, we found that deleting *Tau* ameliorated the loss of NeuN+ neurons and synapses, and the decreased cortical and striatal volume in BACHD mice (Fig. 6 and 7). Interestingly, though little is known about the correlation between specific neuropathological features and the development of behavioral deficits in HD, synaptic loss is the best established neuropathological correlate of cognitive deficits in AD (Coleman and Yao, 2003). Our findings that deleting *Tau* improves neuropathology, as well as some behavioral deficits, strongly validate TAU as a potential target for HD.

In addition to validation of TAU as a therapeutic target in HD, several important implications follow from our studies. Our observation that deleting *Tau* almost fully reverses neuropathology

without correcting motor symptoms adds to the body of work suggesting that neuronal dysfunction, rather than frank neurodegeneration, may underlie some behavioral deficits, especially in the earlier stages of the disease (Van Raamsdonk et al., 2005a, 2005b; Nguyen et al., 2006; Carroll et al., 2011). Furthermore, the beneficial effects of *Tau* deletion on cognitive and affective deficits without amelioration of motor deficits are particularly interesting, especially since frank *TAU* mutations also produce cognitive and emotional deficits in frontotemporal dementia (Spillantini and Goedert, 2013). Together, these results suggest that different symptoms of HD may be caused by changes in different pathways, which would impose some limits on a unifying mechanistic hypothesis behind the development of HD. This interpretation is also supported by a study which showed that neither cognitive scores nor striatal measurements are correlated and fully redundant with the clinical motor examination in HD patients (Paulsen et al., 2008).

The mechanism by which removing endogenous TAU improves mHTT-induced behavioral deficits and neuropathology remains unknown. Localization of TAU in mHTT aggregates was reported in the brain of one patient (Caparros-Lefebvre et al., 2009), but the significance of this finding is unclear as TAU pathology is not widely reported in HD. Although there is no evidence suggesting a direct physical interaction between TAU and HTT, these two proteins interact with components of the post-synaptic density, such as post-synaptic density protein PSD-95 (Sun et al., 2001; Ittner et al., 2010), microtubules and vesicular structures (Smith et al., 2009; Morris et al., 2011b), and protein kinase C and casein kinase substrate in neurons protein 1 (PACSIN1), which has been implicated in synaptic vesicle recycling (Modregger et al., 2002; Liu et al., 2012; Marco et al., 2013). Thus, HTT and TAU may be involved in some of the same protein complexes and molecular pathways.

The beneficial effects of deleting *Tau* in HD may instead be related to the known roles of TAU in axonal trafficking or network excitability and the intersection of these functions with pathogenic mechanisms in HD. Similar to AD, impaired mitochondrial trafficking along axons has been reported in HD (Trushina et al., 2004; Orr et al., 2008; Shirendeb et al., 2012). Since reducing TAU prevented A β -induced impairments in axonal transport of mitochondria in an AD *in vitro* model (Vossel et al., 2010), it may also act similarly in HD. However, the significance of impaired axonal mitochondrial trafficking in pathogenesis of either disorder is unclear. Alternatively, deletion of *Tau* has been shown to correct network hyper-excitability in AD models (Ittner et al., 2010; Roberson et al., 2007, 2011), and *Tau* deletion may act similarly to confer the benefits we observed in BACHD mice. While the negative results from clinical trials blocking glutamate release or NMDARs in HD patients and some animal models (Kremer et al., 1999; Landwehrmeyer et al., 2007; Tallaksen-Greene et al., 2010), have cast doubt on the excitotoxicity hypothesis, excitotoxicity may still have an important role in HD. First, the timing of intervention might be particularly important. Indeed, several studies have suggested that biphasic and stage-dependent changes occur in glutamate transmission, such that activity is increased early and then decreased later in the course of the disease (Hansson et al., 2001; Joshi et al., 2009; André et al., 2011). Second, given the essential function of NMDAR signaling in normal brain function, broad reduction of NMDAR signaling may cause both beneficial and detrimental effects and, thus, may not be the best target. Supporting this, several recent studies have suggested opposing effects of synaptic and extra-synaptic glutamate signaling in HD (Okamoto et al., 2009; Raymond et al., 2011; Dau et al., 2014). Importantly, deleting *Tau* has been proposed to correct cognitive deficits, at least in AD model mice, by blocking disease-

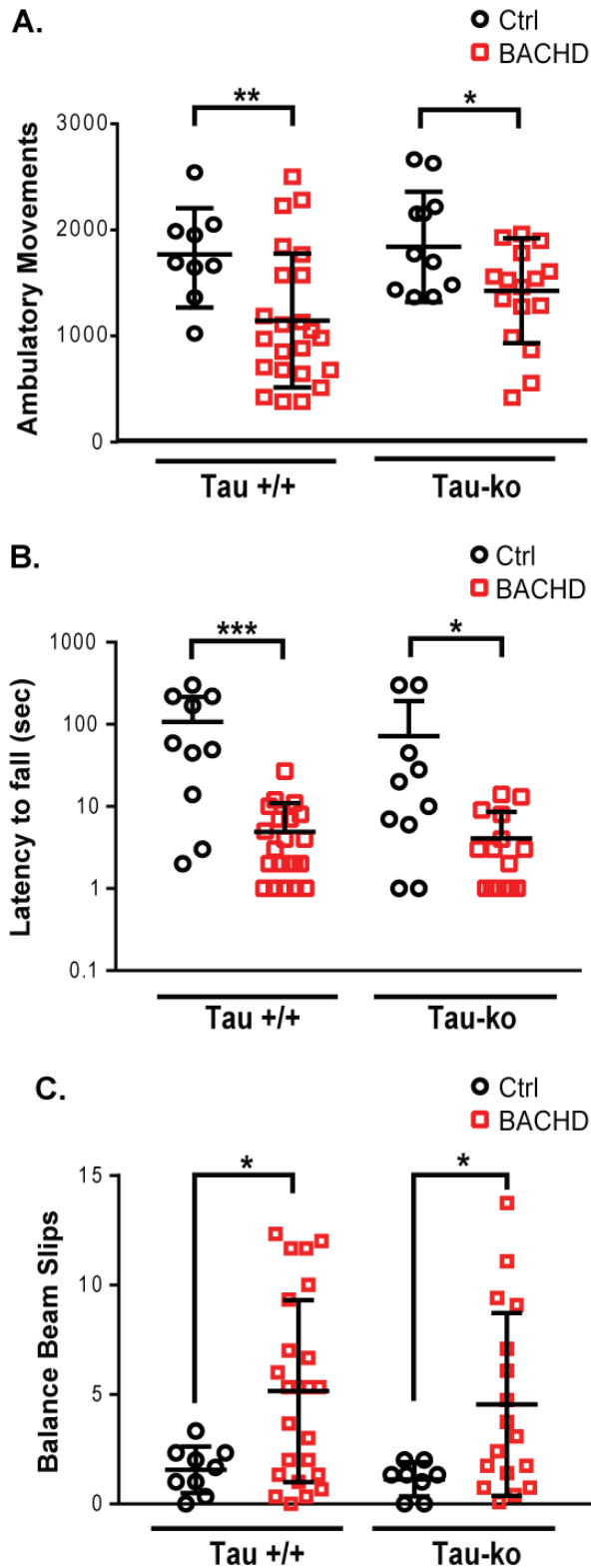
related hyper-excitability without affecting normal synaptic transmission (Roberson et al., 2007; Ittner et al., 2010), which might explain its beneficial effects in the BACHD model.

Regardless of the exact mechanism by which deleting *Tau* confers benefits, the results of our study suggest that HD and AD might have more in common than previously recognized and may share common pathways with respect to cognitive and affective symptoms and neuropathology. Among the neurodegenerative disorders in which the effects of deleting *Tau* were examined, the permissive role of TAU appears specific to AD and HD. Indeed, deleting *Tau* did not prevent deficits in models of several other neurodegenerative disorders, including two mouse models of Parkinson's disease (PD) (Morris et al., 2011a), and a mutant SOD1 expressing mouse model of amyotrophic lateral sclerosis (ALS) (Roberson et al., 2011). In fact, *Tau* deletion even exacerbated some deficits in a model of Niemann-Pick disease type C (Pacheco et al., 2009). However, even though cognitive deficits are also found in Niemann-Pick disease type C (Võikar et al., 2002) and PD (Aarsland et al., 2011), these studies did not specifically examine the effect of deleting *Tau* on the development of cognitive deficits in these models. Therefore, we cannot exclude the possibility that *Tau* deletion may mitigate cognitive deficits, but not other symptoms, caused by several distinct diseases.

Future studies are needed to address several remaining questions. First, the level of TAU reduction required to achieve benefits in HD is not known. In AD models, partial and complete reduction of TAU is sufficient to improve symptoms (Roberson et al., 2007). However, our study examined the effects of complete knock out of *Tau* in the BACHD model and, therefore, does not address this issue. Second, deleting *Tau* from conception in our study precludes us from knowing whether reducing TAU at a later stage would also be beneficial. Alternatively, the protective effects may require the developmental absence of *Tau* and the adaptations that may

result from its absence. Nonetheless, our results suggest that the development of therapies aimed at reducing TAU for treatment of AD may also be useful in treating cognitive and psychiatric symptoms in HD patients and as a cell-preserving therapy.

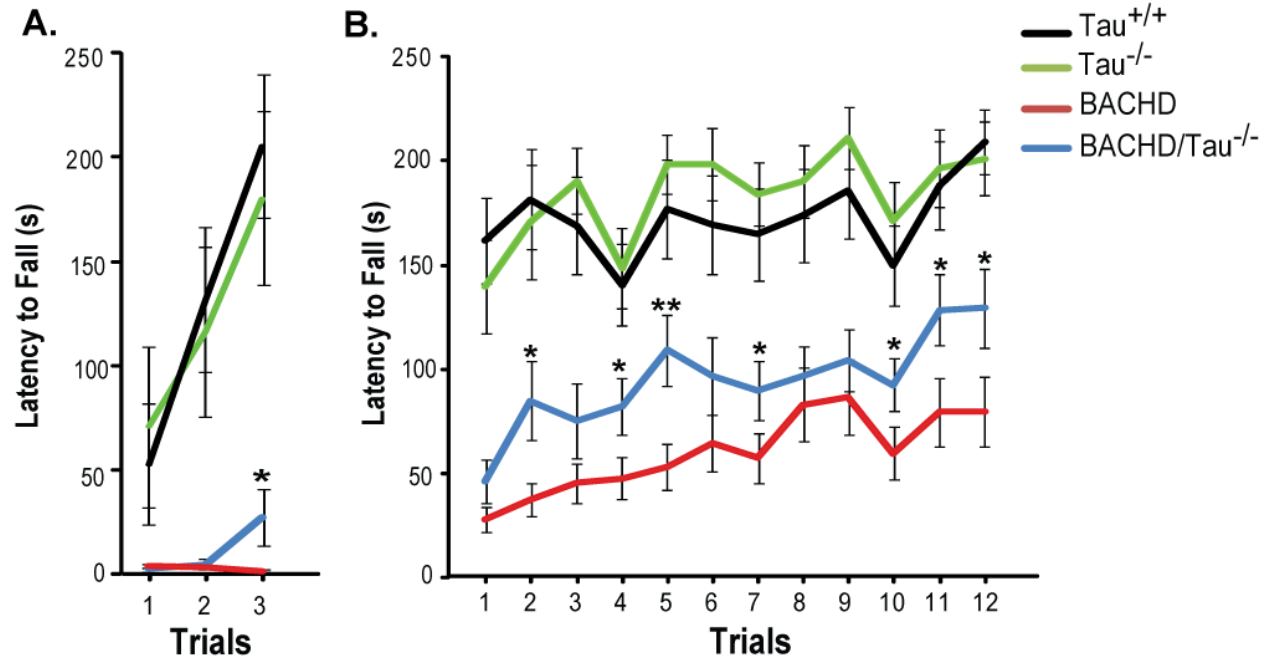
Figure 1. Deleting *Tau* does not significantly alter BACHD-induced motor deficits.



A. Ambulatory movements in the open field were reduced in BACHD mice regardless of *Tau* level ($F_{(1, 54)} = 13.36, p = 0.0006$ for BACHD effect; $F_{(1, 54)} = 1.112, p = 0.2956$ for *Tau* effect; and $F_{(1, 54)} = 0.1053, p = 0.7469$ for interaction by two-way ANOVA, followed by Sidak's multiple comparisons post-tests: BACHD vs. WT: $p = 0.0123$; BACHD/*Tau-ko* vs. *Tau-ko*: $p = 0.0470$; *Tau-ko* vs. WT $p = 0.8820$; BACHD/*Tau-ko* vs. BACHD $p = 0.4198$). **B.** Baseline latency to fall off fixed-speed rotarod was reduced in the BACHD group regardless of *Tau* level ($F_{(1, 55)} = 20.63, p < 0.0001$ for BACHD effect; $F_{(1, 55)} = 1.026, p = 0.3154$ for *Tau* effect; and $F_{(1, 55)} = 0.934, p = 0.3380$ for interaction by two-way ANOVA, followed by Sidak's multiple comparisons post-tests: BACHD vs. WT: $p = 0.0003$; BACHD/*Tau-ko* vs. *Tau-ko*: $p = 0.0271$; *Tau-ko* vs. WT $p = 0.4010$; BACHD/*Tau-ko* vs. BACHD $p = 0.9990$). **C.** Balance beam slips were increased in BACHD and were unaffected by *Tau* deletion ($F_{(1, 54)} = 11.39, p = 0.0014$ for

BACHD effect; $F_{(1, 54)} = 0.5313$, $p = 0.469$ for *Tau* effect; and $F_{(1, 54)} = 0.00499$, $p = 0.944$ for interaction by two-way ANOVA after square-root transformation, followed by Sidak's multiple comparison post-tests: BACHD vs. WT: $p = 0.0346$; BACHD/*Tau*-ko vs. *Tau*-ko: $p = 0.0465$; *Tau*-ko vs. WT $p = 0.867$; BACHD/*Tau*-ko vs. BACHD $p = 0.797$). * $p < 0.05$, ** $p < 0.01$, *** $p < 0.001$. Error bars represent SD. N = 9 for WT (*Tau*^{+/+}:Ctrl); n = 23 for BACHD; n = 9 for *Tau*-ko; n = 17 for BACHD/*Tau*-ko.

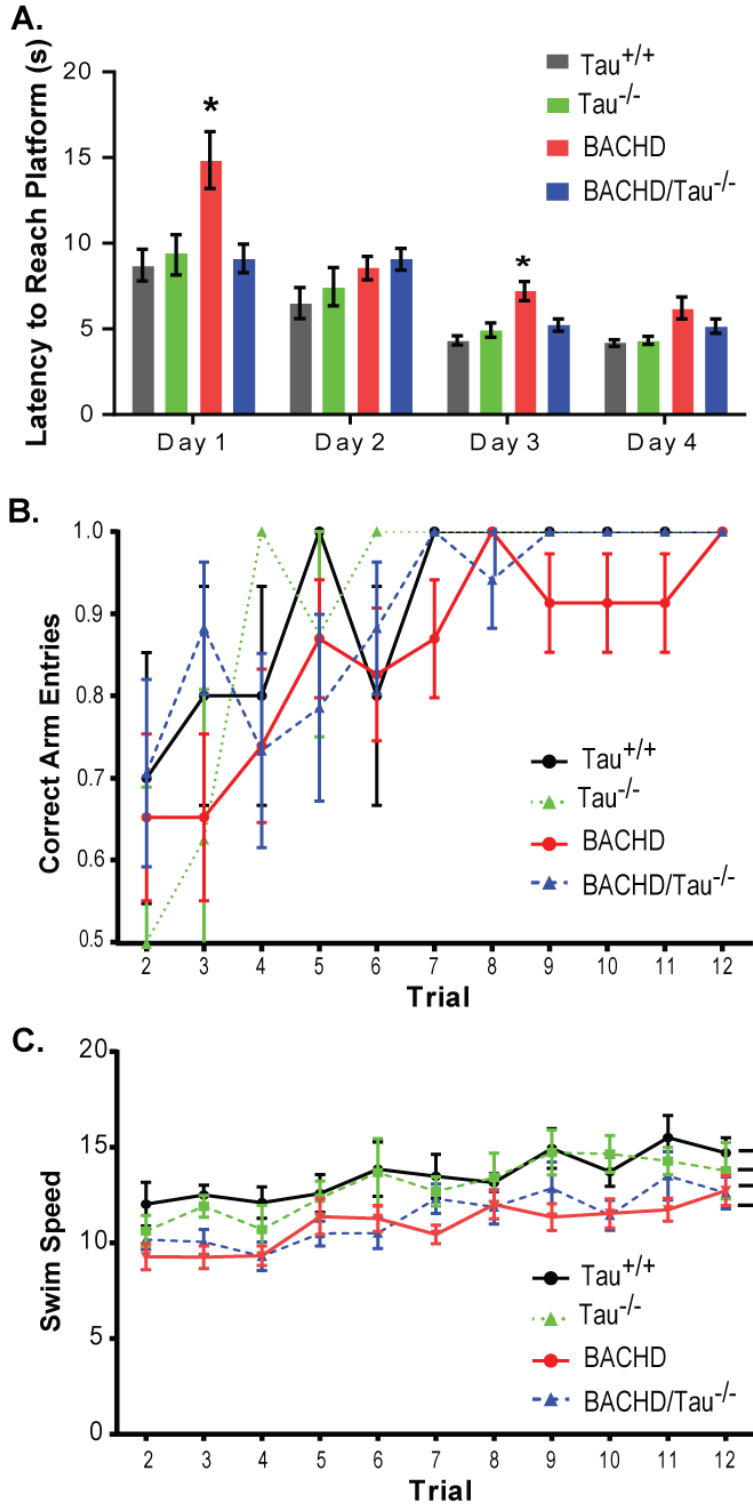
Figure 2. Deleting *Tau* significantly reduces BACHD-induced motor skill learning deficits in the rotarod test.



A, BACHD mice failed to improve during the three trials at fixed speed, while WT and *Tau*-ko mice improved significantly over those trials ($F_{(3, 162)} = 39.61, p < 0.0001$ for genotype effect; $F_{(2, 162)} = 8.093, p = 0.0004$ for trial effect; and $F_{(6, 162)} = 1.966, p = 0.0734$ for interaction by two-way ANOVA, followed by Tukey's multiple comparisons post-tests for main genotype effect: BACHD vs. WT: $p < 0.0001$; BACHD/*Tau*-ko vs. *Tau*-ko: $p < 0.0001$; WT vs. *Tau*-ko: $p = 0.5507$). *Tau* deletion in BACHD mice improved latency to fall by the third trial (BACHD vs. BACHD/*Tau*-ko: $p = 0.0464, DF=36$). **B**, After switching mice onto the accelerated rotarod paradigm, (4–40 rpm; +4rpm per 30 s), WT and *Tau*-ko mice continued to perform similarly near their maximal capacity (Tukey's multiple comparison test of WT vs *Tau*-ko: $p = 0.5187$). BACHD mice, regardless of *Tau* level, started out with similar latency to fall, which was significantly reduced compared to controls (Tukey's multiple comparison test of WT or *Tau*-ko

vs. BACHD: $p < 0.0001$; WT or *Tau*-ko vs. BACHD/*Tau*-ko: $p < 0.001$; BACHD vs. BACHD/*Tau*-ko : $p = 0.8032$). However, BACHD/*Tau*-ko mice improved more than BACHD mice over multiple trials (indicated with asterisks). * $p < 0.05$, ** $p < 0.01$, *** $p < 0.001$, **** $p < 0.001$. Error bars represent SEM. N = 10 for WT; n = 23 for BACHD; n = 10 for *Tau*-ko; n = 16 for BACHD/*Tau*-ko.

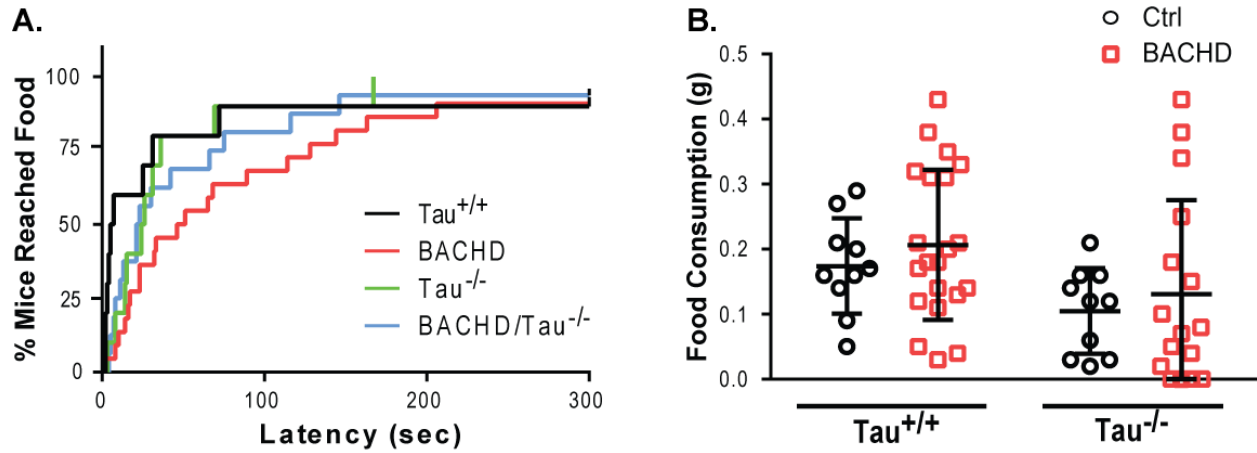
Figure 3. Deleting *Tau* significantly reduces BACHD-induced deficits in procedural learning in the water T-maze test.



A, Latency to reach the platform in the water T-maze was increased in BACHD. Deleting *Tau* alone had no effect, but reduced the BACHD-induced increase in latency ($F_{(3,204)} = 10.66, p < 0.0001$ for genotype effect; $F_{(3,204)} = 25.62, p < 0.0001$ for trial effect; and $F_{(9,204)} = 2.124, p = 0.0290$ for interaction by two-way ANOVA; followed by Tukey's multiple comparison post-tests for main genotype effect: WT vs. *Tau*-ko: $p = 0.9024$; WT or *Tau*-ko vs. BACHD: $p < 0.0011$; WT or *Tau*-ko vs. BACHD/*Tau*-ko: $p > 0.3363$; BACHD vs. BACHD/*Tau*-ko: $p = 0.0018$). **B**, Correct arm entries were quantified. Initially, all groups

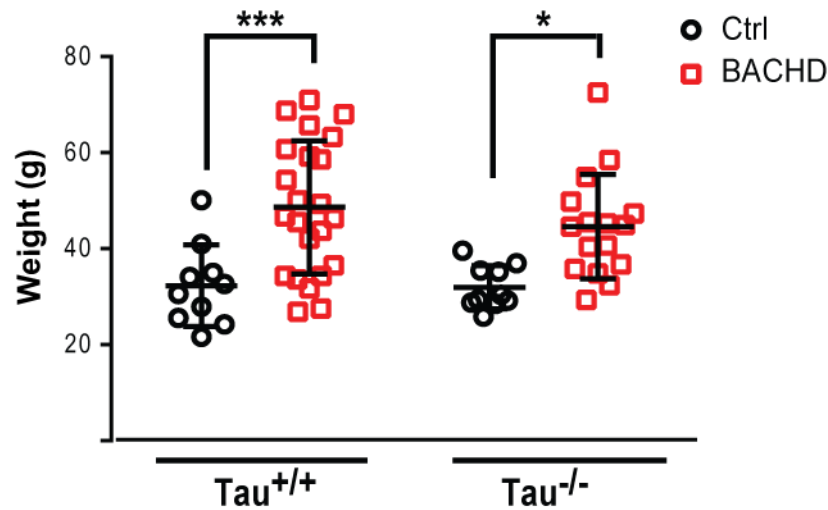
demonstrated a chance level of selecting the correct arm to swim down to reach the platform. By the third and fourth day (trials 7–12), WT and *Tau*-ko mice swam down the correct arm in all trials, whereas BACHD mice initially chose the wrong arm in a few trials. BACHD/*Tau*-ko mice made significantly fewer errors compared to the BACHD mice (trials swimming down incorrect arm during the third and fourth day: WT, 0 of 60 trials; *Tau*-ko, 0 of 48 trials; BACHD, 9 of 138 trials; BACHD/*Tau*-ko, 1 of 102 trials; Fisher's exact test between BACHD and BACHD/*Tau*-ko $p = 0.047$). Error bars represent SEM. **C**, Swim speed in the water T-maze was decreased in the BACHD group regardless of *Tau* level ($F_{(3, 581)} = 18.92, p < 0.0001$ for genotype effect; $F_{(10, 581)} = 6.052, p < 0.0001$ for trial effect; and $F_{(30, 581)} = 0.465, p = 0.9939$ for interaction by two-way ANOVA; followed by Tukey's multiple comparison post-tests for main genotype effect: WT vs. *Tau*-ko: $p = 0.7235$; WT or *Tau*-ko vs. BACHD: $p < 0.0001$; WT or *Tau*-ko vs. BACHD/*Tau*-ko: $p < 0.0011$; BACHD vs. BACHD/*Tau*-ko: $p = 0.5171$). * $p < 0.05$, ** $p < 0.01$, *** $p < 0.001$, **** $p < 0.001$. Error bars represent SEM. N = 10 for WT; n = 23 for BACHD; n = 10 for *Tau*-ko; n = 16 for BACHD/*Tau*-ko.

Figure 4. Deleting *Tau* reduces BACHD-induced anxiety-like symptoms.



A, Latency to approach food was increased in the BACHD group and deleting *Tau* partially reduced this deficit (Kaplan-Meier Analysis: Gehan-Breslow-Wilcoxon $p = 0.0144$ for BACHD vs. WT; Gehan-Breslow-Wilcoxon $p = 0.9792$ for BACHD/*Tau*-ko vs. *Tau*-ko). **B**, Post-test food consumption in the home cage was slightly reduced by deleting *Tau*, regardless of BACHD status ($F_{(1,53)} = 0.886$, $p = 0.3564$ for BACHD effect; $F_{(1,53)} = 5.359$, $p = 0.0245$ for *Tau* effect, and $F_{(1,53)} = 0.0126$, $p = 0.9109$ for interaction by two-way ANOVA after square-root transformation, followed by Sidak's multiple comparison post-tests: BACHD vs. WT: $p = 0.7010$; BACHD/*Tau*-ko vs. *Tau*-ko: $p = 0.8189$; *Tau*-ko vs. WT $p = 0.3211$; BACHD/*Tau*-ko vs. BACHD $p = 0.0912$). * $p < 0.05$, ** $p < 0.01$, *** $p < 0.001$. Error bars represent SD. N = 9 for WT; n = 23 for BACHD; n = 9 for *Tau*-ko; n = 17 for BACHD/*Tau*-ko.

Figure 5. Deleting *Tau* does not alter body weight in mice.



Body weight is increased in the BACHD group regardless of *Tau* level (two-way ANOVA $F_{(1, 55)} = 22.07$, $p < 0.0001$ for BACHD effect; $F_{(1, 55)} = 0.5052$, $p = 0.4802$ for *Tau* effect; and $F_{(1, 55)} = 0.3541$, $p = 0.5542$ for interaction. Sidak's multiple comparisons post-tests: BACHD vs. WT: $p = 0.0006$; BACHD/*Tau*-ko vs. *Tau*-ko: $p = 0.0135$; *Tau*-ko vs. WT $p = 0.9968$; BACHD/*Tau*-ko vs. BACHD $p = 0.4701$). * $p < 0.05$, ** $p < 0.01$, *** $p < 0.001$. Error bars represent SD. N = 10 for WT; n = 23 for BACHD; n = 10 for *Tau*-ko; n = 16 for BACHD/*Tau*-ko.

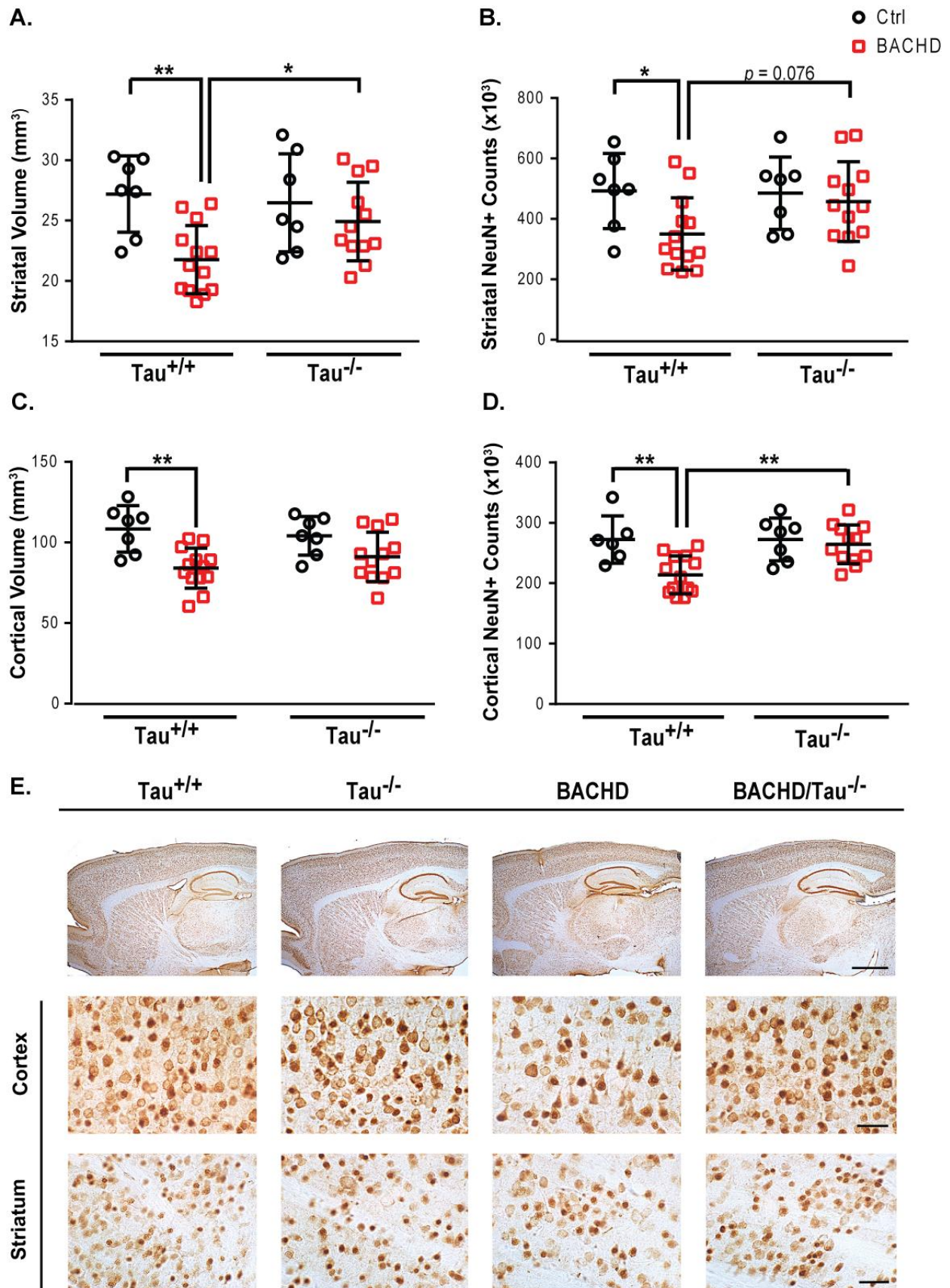
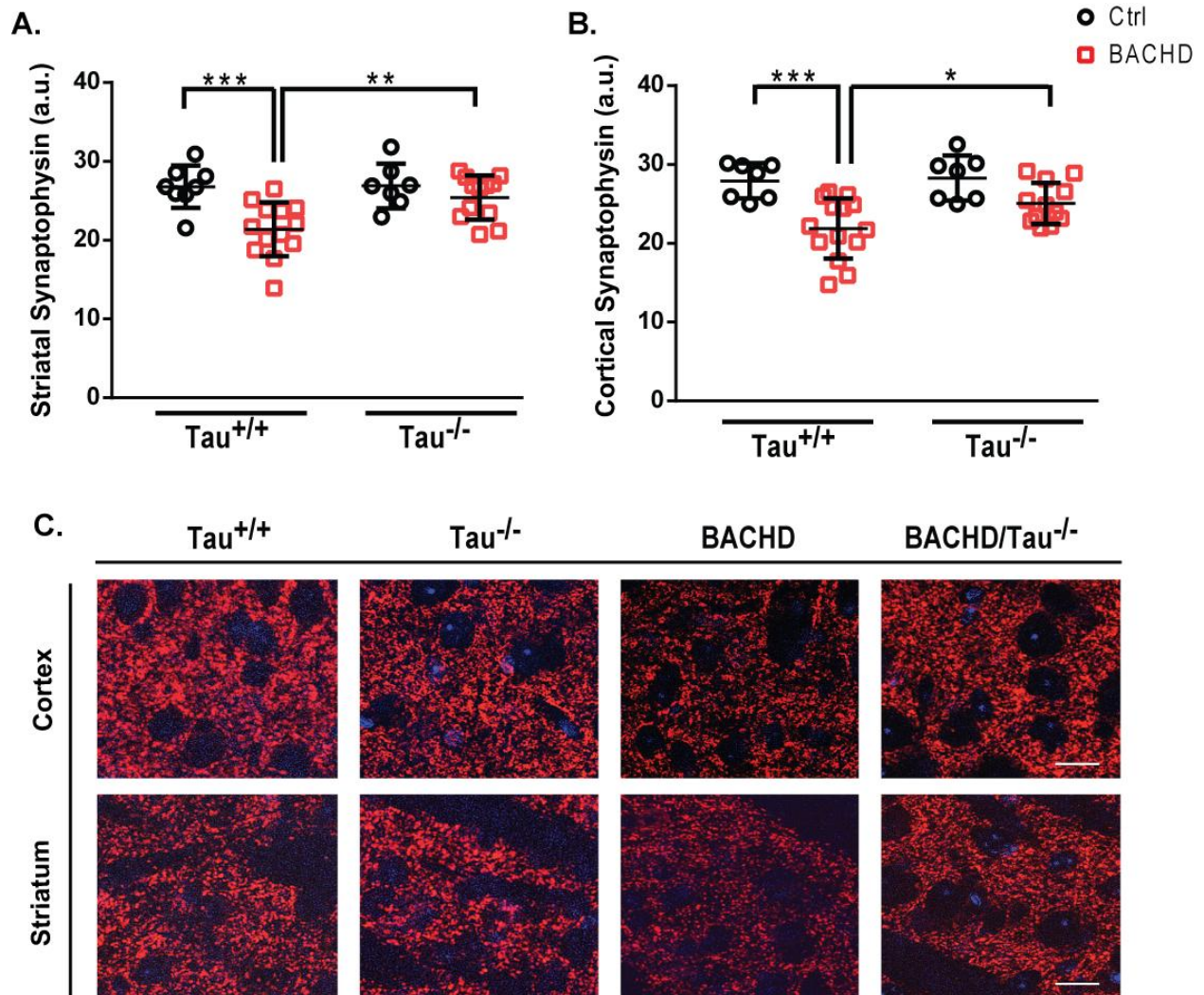


Figure 6. Deleting *Tau* significantly reduces BACHD-induced striatal and cortical pathology.

A, Striatal volume was reduced in BACHD mice, and reversed by deleting *Tau* ($F_{(1,35)} = 10.32, p = 0.0028$ for BACHD effect; $F_{(1,35)} = 1.249, p = 0.271$ for *Tau* effect; and $F_{(1,35)} = 3.199, p = 0.0824$ for interaction by two-way ANOVA, followed by Sidak's multiple comparisons post-tests: BACHD vs. WT: $p = 0.0022$; BACHD/*Tau*-ko vs. *Tau*-ko: $p = 0.5434$; *Tau*-ko vs. WT: $p = 0.896$; BACHD/*Tau*-ko vs. BACHD: $p = 0.0409$). **B**, The number of striatal NeuN+ cells was reduced in BACHD mice and deleting *Tau* reduced this deficit ($F_{(1,35)} = 4.178, p = 0.0485$ for BACHD effect; $F_{(1,35)} = 1.440, p = 0.238$ for *Tau* effect; and $F_{(1,35)} = 1.881, p = 0.179$ for interaction by two-way ANOVA, followed by Sidak's multiple comparison post-tests: BACHD vs. WT: $p = 0.0401$; BACHD/*Tau*-ko vs. *Tau*-ko: $p = 0.8703$; *Tau*-ko vs. WT: $p = 0.9928$; BACHD/*Tau*-ko vs. BACHD: $p = 0.0764$). **C**, Cortical volume was reduced in BACHD mice and deleting *Tau* showed a trend towards reduced this deficit ($F_{(1,35)} = 16.70, p = 0.0002$ for BACHD effect; $F_{(1,35)} = 0.08524, p = 0.772$ for *Tau*; and $F_{(1,35)} = 1.519, p = 0.2260$ for interaction by two-way ANOVA, followed by Sidak's multiple comparisons post-tests: BACHD vs. WT: $p = 0.0011$; BACHD/*Tau*-ko vs. *Tau*-ko: $p = 0.103$; *Tau*-ko vs. WT: $p = 0.807$; BACHD/*Tau*-ko vs. BACHD: $p = 0.379$). **D**, The number of cortical NeuN+ cells was reduced in BACHD mice and deleting *Tau* reduced this deficit ($F_{(1,34)} = 8.399, p = 0.0065$ for BACHD effect; $F_{(1,34)} = 4.879, p = 0.034$ for *Tau* effect; and $F_{(1,34)} = 4.787, p = 0.0356$ for interaction by two-way ANOVA, followed by Sidak's multiple comparison post-tests: BACHD vs. WT: $p = 0.0024$; BACHD/*Tau*-ko vs. *Tau*-ko: $p = 0.8496$; *Tau*-ko vs. WT: $p = 0.9999$; BACHD/*Tau*-ko vs. BACHD: $p = 0.0013$). * $p < 0.05$, ** $p < 0.01$, *** $p < 0.001$, **** $p < 0.001$. Error bars represent SD. N = 7 for WT (*Tau*^{+/+}:Ctrl); n = 13 for BACHD; n = 7 for *Tau*-ko; n = 12 for

BACHD/*Tau*-ko. *E*, Representative images of NeuN staining of the cortex and striatum (upper panel: scale bar size = 250 μ ; lower panel scale bars = 25 μ).

Figure 7. Deleting *Tau* significantly improves the BACHD-induced loss of synaptophysin immunoreactivity.



A, Striatal synaptophysin immunoreactivity was reduced in BACHD mice and deleting *Tau* reduced this deficit ($F_{(1, 36)} = 12.26$, $p = 0.0013$ for BACHD effect; $F_{(1, 36)} = 4.371$, $p = 0.0437$ for *Tau* effect; and $F_{(1, 36)} = 4.016$, $p = 0.0527$ for interaction by two-way ANOVA, followed by Sidak's multiple comparisons post-tests: BACHD vs. control WT: $p = 0.0006$; BACHD/*Tau*-ko vs. *Tau*-ko: $p = 0.5239$; *Tau*-ko vs. WT: $p = 0.9981$; BACHD/*Tau*-ko vs. BACHD: $p = 0.0038$).

B, Cortical synaptophysin immunoreactivity was reduced in BACHD mice and deleting *Tau*

reduced this ($F_{(1, 36)} = 20.63$, $p < 0.0001$ for BACHD effect; $F_{(1, 36)} = 2.973$, $p = 0.0933$ for *Tau* effect; $F_{(1, 36)} = 1.885$, and $p = 0.1783$ for interaction by two-way ANOVA, followed by Sidak's multiple comparison post-tests: BACHD vs. WT: $p = 0.0003$; BACHD/*Tau*-ko vs. *Tau*-ko: $p = 0.0658$; *Tau*-ko vs. WT: $p = 0.9706$; BACHD/*Tau*-ko vs. BACHD: $p = 0.0259$). * $p < 0.05$, ** $p < 0.01$, *** $p < 0.001$, **** $p < 0.001$. Error bars represent SD. N = 7 for WT (*Tau*^{+/+}:Ctrl); n = 13 for BACHD; n = 7 for *Tau*-ko; n = 12 for BACHD/*Tau*-ko. **E**, Representative images of synaptophysin staining of the cortex and striatum (upper panel scale bars = 250 μ ; lower panel scale bars = 10 μ).

Chapter 3: Down-regulation of ACTN2 in the BACHD mouse model of Huntington's disease

Introduction

Transcriptional dysfunction is hypothesized to play a major role in HD and other polyglutamine diseases (Cha, 2000; Sugars and Rubinsztein, 2003; Seredenina and Luthi-Carter, 2012). Transcriptional changes have been observed in striata of HD patients (Hodges et al., 2006) and several HD mouse models (Chan et al., 2002; Desplats et al., 2006; Kuhn et al., 2007; Mazarei et al., 2009; Becanovic et al., 2010; Thomas et al., 2011), in isolated mHTT-expressing cells in culture (Sipione et al., 2002; Runne et al., 2008), and in human neural stem cells derived from induced pluripotent stem cells of HD patients (The HD iPSC Consortium, 2012).

Genes for which changes have been detected at the RNA level are diverse and include those important for neuronal function such as neurotransmitter receptors, intracellular signaling molecules and second messengers, cytoskeletal proteins, and synaptic organization and release proteins. Nonetheless, the functional significance of these changes remains largely unknown. First, the degree to which large-scale transcriptional dysregulation is a direct result of mHTT expression instead of neurodegenerative changes to tissue architecture and composition is unclear. The study by Hodges and colleagues (Hodges et al., 2006) suggested that gene expression changes are not strictly the result of cell loss or changes in tissue architecture. In contrast, studies in the YAC models—that express full-length mHTT and show behavioral deficits, but lack prominent neurodegeneration as a feature until late in the disease—have identified fewer transcriptional changes, suggesting that large-scale perturbations in mRNA levels are not required for the development of the neurologic phenotypes observed in these

models (Chan et al., 2002). Furthermore, the change in transcript level for any given gene may be etiologic and mediate toxic effects, a correlative epiphenomenon, or an adaptive homeostatic response by the cell or organism to the disease insult.

While the BACHD model is commonly used to study disease mechanisms and therapeutic strategies in HD, the presence and degree of transcriptional dysfunction in this model is unknown. To address this, we set out to compare the transcriptional profile of BACHD and WT mice at 8 months, an age when these mice show robust behavioral manifestations of HD without significant neuropathology (Gray et al., 2008). We used the recently developed RNA-Seq approach which provides a high-throughput, unbiased, and more precise quantitative measurement of levels of transcripts and their isoforms (Wang et al., 2009), with the hopes of better understanding the contribution of transcriptional dysfunction to this important model of HD.

Materials and Methods

Plasmids

ACTN2-GFP and ACTN2-mApple were derived from Mammalian expression vector containing actinin, alpha 2 (ACTN2) (cDNA-clone ID: HsCD00445606 from DNAsu) and subcloned into pGW1-CMV (British Biotechnologies). The HTT constructs (HTT-N586) with 17 or 136 polyQ repeats were cloned into pGW1-GFP or pGW1-mApple from full-length HTT constructs JM031 and JM032 (gift from Ray Truant McMaster University, ON Canada). All constructs were

verified by sequencing. In co-transfection experiments, we used pGW1-GFP or pGW1-mApple as a survival marker.

Mouse Model

For the RNA-Seq study, BACHD mice and their control littermates on an FVB background (Gray et al., 2008) were group housed with a normal light–dark cycle in a specific pathogen-free facility and with *ad libitum* access to food and water. All experiments were approved by the Committee on Animal Research of the University of California, San Francisco (Approval Number AN087648-03B).

RNA extraction and RNA-Seq

36-week old BACHD mice and their WT littermates were maintained undisturbed in their home cage until immediately prior to extraction. Three age- and sex-matched mice (2 females, 1 male) of each genotype were anesthetized with isoflurane and decapitated with a sharp pair of scissors. Brains were removed, dissected on ice, snap frozen in liquid nitrogen, and stored at -80 C until use. Frozen tissues (striatum, cortex, or cerebellum) were disrupted and homogenized with the TissueLyser II (Qiagen, Germantown, MD) and total RNA was isolated using the miRNeasy Mini kit (Qiagen, Germantown, MD), according to the manufacturer's instructions. On-column DNase I digestion was performed to eliminate trace contamination with genomic DNA.

The RNA quality was checked using Agilent 2100 Bioanalyzer (Agilent, Santa Clara, CA, USA) on all samples before pooling samples of a given genotype together. Only samples with RNA integrity number (RIN) between 9.5-10 were used. 75-bp single-end RNA sequencing (RNA-Seq) was performed on the Illumina Genome analyzer II following the manufacturer's suggestion (Illumina, San Diego, CA), as previously described (Chen et al., 2012). Briefly, 1 µg high-quality

RNA was used to enrich poly-adenylated RNA, which was then fragmented and reverse transcribed, followed by the synthesis of the second strand. Each resulting double-stranded cDNA fragment was blunt-ended, adenylated, ligated to adaptors, and size-purified for ~200-bp fragments. These size-selected cDNA templates were further enriched using PCR and checked for quality on the Agilent 2100 Bioanalyzer (Agilent, Santa Clara, CA, USA). 75-bp sequencing was performed using the SBS sequencing kit v2 (Illumina, San Diego, CA, USA). One lane was used for each sample. Greater than 28 million reads were obtained per sample, of which > 92% were high-quality (HQ) filtered reads. Reads were analyzed and mapped via the TopHat program (Trapnell et al., 2009). More than 22 million mapped reads were obtained for each sample.

Quantitative Real Time PCR (qRT-PCR)

The same RNA samples used for RNA-Seq plus some additional brains (6 in total) were used for qRT-PCR. 20ng of RNA was converted to cDNA using the Taqman Reverse Transcription kit (Invitrogen) using a 1:1 mix of random hexamers and oligo dT. qRT-PCR was performed by the Sybr Green method (Applied Biosystems) on 1:40 dilutions of the samples using a 7900HT Fast Real-Time PCR system (Applied Biosystems).

Gene specific primers were selected from the Mouse Primer Depot database (<http://mouseprimerdepot.nci.nih.gov/>) and verified for quality and specificity using the dissociation curve method before use. The sequence of the primers were as follows:

HTT-F: 5'-ATC CCG GTC ATC AGC GAC TAT C-3'

HTT-R: 5'-GCT TGT AAT GTT CACGCA GTG G-3'

Actn2-F: 5'-ATG ATC CAG GAG GAG GAG TG-3'

Actn2-R: 5'-TCG ATG TTC TCG ATC TGG GT-3'

Penk-F: 5'-TAA ATG CAG CTA CCG CCT G-3'

Penk-R: 5'-TGT TAT CCC AAG GGA ACT CG-3'

Gad2-F: 5'-CAG CCT TAG GGA TTG GAA CA-3'

Gad2-R: 5'-CCA GGA AAG GAA CAA ATC CT-3'

Snpr-F: 5'-CTG AAG GGA ACT GGT TCG AG-3'

Snpr-R: 5'-CAA ATG CAA ACA TTG CAA AAA-3'

Scg2-F: 5'-GAA ATG ATC AGG GCT TTG GA-3'

Scg2-R: 5'-CTC TCT GCC AAG TGG CTT TC-3'

Mouse *Gad1*, *Slc30a3*, *Dlx1*, and *Calb2* primers were purchased from Qiagen (SYBR Green-based QuantiTect Primer Assay) and verified before use.

Mouse beta-actin (*Actb*: QuantiTect primers, Qiagen) was used to normalize samples. Relative transcript abundances were analyzed from Ct values using the standard curve method.

Immunocytochemistry

Cortical and striatal rat neurons were grown on 96-well plates or 12 mm cover-slips. Neurons were fixed, at various intervals after plating, in 4% PFA + 4% sucrose and immunocytochemistry was performed as described (Saudou et al., 1998). Cells were labeled with the following antibodies: mouse anti-ACTN2 (1:1500; Sigma-Aldrich, clone EA-53), mouse anti-MAP2 (1:500; Millipore, MAB3418), rabbit anti-DARPP32 antibody (1:200; Santa Cruz, sc-11365).

Primary antibody staining was followed by staining with the species-appropriate secondary antibodies: anti-rabbit Cy3 or Cy5, or anti-mouse Cy3 or Cy5 (1:250; Jackson Immunochemical).

Western blot analysis

For experiments analyzing ACTN2 protein levels, brains were harvested from 1-yr-old BACHD mice or their WT littermates, dissected on ice, snap frozen on dry ice, and stored at -80 C until further use. Striata were homogenized using a pellet pestle (Kontes) in a modified RIPA buffer (50 mM Tris-Cl, pH 7.4, 150 mM NaCl, 0.5% deoxycholate, 1% NP-40 and 0.1% SDS) supplemented with Halt Protease (Thermo-Fischer Scientific). The homogenates were then centrifuged at 4 C for 15 min at 13,000 rpm and the soluble supernatant was stored.

Protein concentration in samples was determined using the BCA Protein Assay (Thermo-Fischer Scientific). Western analysis was then carried out by loading equal amounts of protein per sample on NuPAGE (Invitrogen) 3-8% Tris-Acetate pre-cast gels. Samples were prepared as recommended by the Nu-PAGE system. After electrophoresis, the samples were transferred to PVDF membranes (Thermo Scientific), which were then blocked with 5% nonfat milk and subsequently incubated with anti-ACTN2 (1:500, overnight at 4°C; Sigma-Aldrich, clone EA-53), anti-HTT (monoclonal antibody 4H7H7; 1:20000), anti- β -actin (1:20000, Sigma-Aldrich), or anti- γ -tubulin (Sigma, T6557, 1:20,000) antibodies. Immunoreactivity was measured by probing with horseradish peroxidase-conjugated anti-rabbit (1:10000, Jackson ImmunoResearch Laboratory) or anti-mouse IgG (1:10000, Calbiochem) followed by exposure to ECL detection reagents (Perkin Elmer).

Cell Culture and Transfection

Primary rat cortical or striatal neurons were dissected from rat pups at embryonic days E20–E21 and cultured in 96-well plates at 0.6×10^6 and 0.7×10^6 cells/ml, respectively. At 5-days *in vitro* (DIV), neurons were transfected with plasmids by Lipofectamine 2000 reagent (Life Technologies, Grand Island, NY), per manufacturer's recommendations. For survival analysis, neurons were cotransfected with a diffuse fluorescent protein marker (pGW1-GFP or pGW1-mApple), WT- or polyQ-expanded- N-terminal fragment of HTT (corresponding to the first 586a amino acids in the human protein) tagged with a fluorescent protein different than the survival marker (pGW1-HTT-N586 tagged with either GFP or mApple), and pGW1-ACTN2 or pGW1-empty vector (0.8–1.2 μ g of total DNA per well). HTT-N586 fragment was chosen for these studies, as it may be a pathologically important product of HTT proteolysis by caspase-6 (Pouladi et al., 2009), and significantly easier to express in primary neurons than the full-length protein. In this model, death is indicated by the loss of the plasma membrane integrity, which is detected as an abrupt loss of expression of the fluorescent transfection marker. This model recapitulates many cellular and molecular features observed in brains from HD patients including polyQ-dependent cell type-specific death and IB formation (identified as foci of intense fluorescence from fluorescently-tagged mHTT), and has predicted aspects of the disease that have later been validated *in vivo* (Arrasate et al., 2004b).

Robotic Microscope Imaging System and Image Analysis

For neuronal survival analysis, images of neurons were taken at 24 h intervals post transfection with a high-throughput automated microscopy platform (Arrasate et al., 2004b; Arrasate and Finkbeiner, 2005; Daub et al., 2009) capable of longitudinally imaging thousands of individual neurons over long periods (i.e. days to months). The images collected from the different experimental group were analyzed in an identical manner. Using custom algorithms written in-

house in Pipeline Pilot (Accelrys, San Diego, CA), the images were background- and shading-corrected by the median background correction method. Live transfected neurons were selected for analysis based on fluorescence intensity, morphology, and presence of extended processes at the start of the experiment. Next, measurements of HTT or ACTN2 expression level and neuronal survival times were extracted from the images. The expression levels of tagged versions of HTT or ACTN2 were estimated by measuring the fluorescence intensity in the appropriate channel over a region of interest that corresponded to the cell soma, using the fluorescence of the co-transfected morphology marker (Arrasate et al., 2004b). Survival times of individual neurons post transfection were determined from the abrupt loss of the diffuse fluorescent protein marker (Arrasate et al., 2004b). The survival times for cohorts of neurons were tabulated and survival curves for the population were constructed as described below.

Statistical Analysis

For analysis of the longitudinal single-cell data collected by tracking individual neurons over time with automated robotic microscopy, survival analysis was used to accurately determine differences in longevity between populations of cells (Jager et al., 2008). The survival time of a neuron was defined as the time point at which the cell was last seen alive. For neurons that lived the entire length of the experiment, survival time was defined as the last time point of the experiment and treated as censored. The survival package for the statistical software R was used to construct Kaplan-Meier curves from the survival data. Survival functions were fitted to these data with Kaplan-Meier analysis and used to derive cumulative hazard (or risk-of-death) curves that describe the instantaneous risk-of-death for individual neurons in the cohort being tracked. Differences in the cumulative risk-of-death curves were assessed with the log rank test.

To determine how much an observed abnormality or microscopic change predicts the monitored outcome, hazards analysis was performed. The instantaneous risk of death (*hazard function*) in a cohort of neurons at any time is calculated mathematically as the limit of the number of events per unit time divided by the number at risk as the time interval decreases. Cox proportional hazard regression analysis was used to generate hazard ratios that quantified the relative risk-of-death between two cohorts of neurons expressing different combination of transfected proteins or the predictive values of variables on the risk of death (Arrasate et al., 2004b; Miller et al., 2011, 2010). The sign and size of the *Cox coefficient* (β) for a measured cellular feature describe, respectively, its predictive relationship to the fate of the cell and the magnitude of its effect. Hazard ratios and their respective *p* values were generated using the *coxph* function in the survival package for the R statistical software (Andersen and Gill, 1982). Cox models were analyzed for violations of proportional hazards and for outlier data points using *cox.zph* and *dfbeta* functions in R, respectively.

To compare differences across two groups, the groups were statistically compared using an unpaired *t*-test or a Mann–Whitney test. To compare differences across groups, groups were statistically compared using one-way ANOVA, followed by post-tests if indicated.

Results

RNA-Seq expression profiling of BACHD mice

To explore the transcriptional profile of BACHD mice compared to their WT littermates, striatal, cortical, and cerebellar mRNAs of BACHD and WT littermates were analyzed using the

sequencing-based RNA-Seq approach (Wang et al., 2009). RNA samples were prepared from 8-month-old age- and gender-matched mice. To account for biological variability, for each genotype and brain region, RNA samples were pooled from 3 mice after ensuring RNA quality. Sequencing reads were mapped using the TopHat2 algorithm (Trapnell et al., 2013) and analyzed by HTSeq (Anders et al., 2014). The details of the sequencing and HTSeq counts are shown in Table 1. As a measure of quality control, we compared the regional specificity of genes in our RNA-Seq dataset with a previously published dataset of genes that show regionally restricted expression in the brain (D'Souza et al., 2008) and found similar regional distributions for all genes identified as regionally enriched in the striatum, cortex, or cerebellum in that dataset.

Comparing BACHD and WT mice, RNA-Seq gene expression counts were highly concordant for striatal, cortical, and cerebellar samples between the two groups (Fig. 8), suggesting that there is little evidence of significant transcriptional dysregulation in the samples from BACHD mice. Furthermore, the brains of BACHD mice did not show changes in RNA counts for striatally enriched genes such as DARPP-32, Dopamine Receptor D1a (Drd1), and Dopamine Receptor D2 (Drd2) that are found to be dysregulated in human HD brains and various other HD mouse models (Table 2), suggesting that changes in the level of these transcripts are not core drivers of the phenotype in these mice.

Nonetheless, the global correlation of RNA-Seq gene expression counts suggested greater changes in the striatum, lesser changes in the cortex, and the least changes in the cerebellum (Fig. 8 and Table 3). Yate's corrected chi-squared analysis revealed a significant difference in the numbers of genes changed among the groups ($\chi^2 = 66.75$, $df = 2$, $p < 0.0001$ for genes expressed and changed > 2-fold). This pattern of changes parallels previous observations in HD brains that the extent of transcriptional dysregulation correlates with the degree of tissue

involvement in the disease (Hodges et al., 2006). Given the design of our study and the lack of sequencing read replicates, we were unable to assign statistical significance to the differences in gene expression between BACHD and WT mice. However, since little to no changes are detected in the cerebellum in HD patients and other mouse models (Seredenina and Luthi-Carter, 2012), we used the variability in the cerebellar samples as a bar for identifying candidate genes whose expression is potentially altered in the striatum and cortex of BACHD mice. From that, we generated a list of candidate genes to further test by quantitative real-time PCR (qRT-PCR) and further prioritized that list based on whether the candidate genes had been previously identified as changed in HD brains in the same direction as the change in our dataset. The candidate genes were then tested by qRT-PCR in a larger set of brain which included the original 3 brains for each sample.

For most of the candidate genes tested, even though the average levels of mRNA from the original 3 brains for each genotype by qPCR matched the RNA-Seq counts (data not shown), those changes were not statistically significant by qRT-PCR upon testing in a larger group of brains (Fig. 9). However, one notable exception was the nearly 50% reduction of α -Actinin 2 (*Actn2*), which we were able to confirm by qRT-PCR (Fig. 10; 95% confidence interval of mean difference between WT and BACHD: -0.3211 to -0.7904).

Effect of ACTN2 on mHTT-induced cell death

Having verified that *Actn2* mRNA is decreased in BACHD mice, we asked whether the mRNA-level changes are also reflected at the level of the protein. As shown in Fig. 11, ACTN2 protein levels were also decreased by 87% in the striatum of 8-month-old BACHD mice as compared to

control littermates (95% confidence interval of mean difference between WT and BACHD: -0.02417 to -0.157).

While down-regulation of *Actn2* mRNA has been observed in human caudate from HD patients (Hodges et al., 2006; Becanovic et al., 2010) and multiple HD mouse models such as the R6/1 (Desplats et al., 2006), R6/2 (Luthi-Carter et al., 2003), N171-98Q (Thomas et al., 2011), and YAC128 model (Becanovic et al., 2010), the functional significance of this alteration is not known. Since our RNA-Seq data suggests that *Actn2* mRNA expression correlates with the pattern of tissue involvement in HD (highest in the striatum, medium in the cortex, and lowest in the cerebellum), we hypothesized that the normally higher expression of ACTN2 in striatal neurons may contribute to pathogenesis in HD and that the down-regulation of ACTN2 may be a compensatory homeostatic response. To this end, we tested the effect of ACTN2 over-expression in a primary cortical culture model of mHTT toxicity which recapitulates key features of HD such as polyQ-dependent IB formation, neuritic dystrophy, and death (Miller et al., 2010).

First, we verified the differential expression of ACTN2 protein in our primary striatal and cortical cultures. By immunohistochemistry, ACTN2 levels are significantly higher in DARPP-32+ striatal primary neurons than cortical neurons (Fig. 12), with little detectable expression in cortical neurons. We then tested the effect of over-expression of ACTN2 on mHTT-dependent toxicity in cortical neurons. To visualize cells expressing ACTN2 in real time, we generated fluorescently tagged full-length human ACTN2 constructs (hACTN2). Primary cortical neurons were transfected with the following combination of constructs: 17Q-HTTN586 + empty vector (EV), 17Q-HTTN586 + hACTN2, 136Q-HTTN586 + EV, and 136Q-HTTN586 + hACTN2, EV + hACTN2. All combinations also included a diffuse survival marker (mApple or EGFP). Starting approximately 24 h after transfection, individual transfected neurons were imaged and

tracked daily for 7 consecutive days by automated imaging (Arrasate and Finkbeiner, 2005). The survival marker was used to track the cell's morphology throughout its lifetime and its abrupt loss was interpreted as death, as previously established (Arrasate et al., 2004b). The time-to-death data from hundreds of neurons were then analyzed by Kaplan-Meier survival analysis, which is widely used in medicine to determine how an observed factor affects the likelihood of an outcome such as death (Hosmer and Lemeshow, 1999). As expected, cortical neurons expressing mHTT (136Q-HTTN586 + EV) had significantly higher cumulative risk of death than cortical neurons expressing non-expanded HTT (17Q-HTTN586 + EV) (Fig. 13). ACTN2-overexpression resulted in a significantly higher cumulative risk of death in neurons co-expressing 17Q-HTT, but no further toxicity of mHTT was observed in the presence of ACTN2 over-expression (Fig. 13A: 136Q-HTT + ACTN2 vs. 17Q-HTT + ACTN2: HR = 1.105; log-rank $p = 0.425$; 136Q-HTT + ACTN2 vs. 136Q-HTT + EV: HR = 1.104; log-rank $p = 0.367$), suggesting an epistatic relationships between ACTN2 and mHTT expression. Since expression levels of mHtt have been show to correlate with cell death (Arrasate et al., 2004), we measured HTT expression levels at 24 hours. Importantly, the expression level of HTT was comparable across all groups (Fig. 13B), suggesting that these effects are not due to differences in expression level of mHTT.

Discussion

We performed sequencing-based genome-wide expression profiling of striatal, cortical, and cerebellar tissues from BACHD and control mice at 8 months of age by RNA-Seq. This analysis revealed little evidence of significant transcriptional dysregulation in the samples from BACHD

mice (Fig. 8 and 9). Notably the brains of BACHD mice, at an age when they exhibit robust behavioral deficits, did not show changes in striatally enriched genes such as *Darpp-32*, *Drd1a*, and *Drd2* that are commonly found to be dysregulated in human HD brains and various other HD mouse models and are thought to be crucial mediators of pathology (Table 2). While the full transcriptional profile of BACHD mice had not previously been investigated, our results agree with and expand upon a previous observation suggesting that the BACHD model exhibits robust behavioral and neuropathological deficits without striatal transcriptional dysregulation (Pouladi et al., 2012). While Pouladi and colleagues only examined a select group of genes by qRT-PCR, we took an unbiased approach using RNA-seq. Together with the study by Pouladi and colleagues, our findings suggest that extensive transcriptional changes are not necessary for the manifestation of mHTT-induced phenotypic deficits that can be seen in the BACHD model, such as motor dysfunction, depressive-like phenotype and neuropathological features. This conclusion is also in agreement with observations in other mouse models of HD. For example, Chan and colleagues (Chan et al., 2002) showed that the HD46, HD100, and YAC72 model mice, even at 12 months, show little transcriptional changes and the few detected changes are only slightly more than the expected false positive rate. Accordingly, some mRNAs identified as changed could not be confirmed by RT-PCR. Data from young R6/2 mice (<6 weeks of age) that are already symptomatic also show a similar lack of large-scale perturbations in mRNA levels (Luthi-Carter et al., 2002), even though older R6/2 mice show significant mRNA changes. A reasonable interpretation of these finding is that large-scale perturbations in mRNA levels are not an integral component of the early stages in HD pathogenesis and are not required for the development of the neurologic phenotypes observed in these HD animal models.

The candidate genes that we chose to validate by qRT-PCR were those for which our RNA-Seq data was suggestive of a change in mRNA levels and there was a precedent or plausible mechanism for their involvement in HD. For example, calretinin/calbindin 2 (Calb2) is a calcium-binding protein with roles in calcium buffering, long-term potentiation, motor coordination, and neuro-protection. It was shown to interact with HTT, its over-expression reportedly reduces mHTT-caused cell death in non-neuronal and neuronal cell cultures, and its down-regulation in inducible neuronal cells enhances mHTT-induced death (Dong et al., 2012). Furthermore Calb2⁺ interneurons are selectively spared in HD patients, even though its expression was found reduced in postmortem striatum from HD patients (Massouh et al., 2008) and in dentate gyrus of R6/2 mice (Fedele et al., 2011). Enkephalins (PENK) are neuropeptides that compete with and mimic the effects of opiate drugs and play a role in a number of physiologic functions, including pain perception and responses to stress, and increasing glutamate release and decreasing GABA concentrations in the striatum. Decreased levels of PENK have been observed in low grade HD brains (Richfield et al., 1995; Sapp et al., 1995; Augood et al., 1996) and multiple mouse models of HD (Luthi-Carter et al., 2000, 2002; Desplats et al., 2006; Kuhn et al., 2007; Runne et al., 2008; Thomas et al., 2011; Pouladi et al., 2012). Distal-less homeobox 1 (Dlx1) is a homeobox transcription factor required for the differentiation, migration, and survival of medium spiny neurons that are among the most affected population of neurons in HD (Anderson et al., 1997). Nonetheless, none of these genes appeared to be changed at the mRNA level in the striata of BACHD mice (Fig. 9).

Of all the genes that we set out to test by qRT-PCR, we were able to confirm only one as changed in BACHD brains: α -actinin-2 (*Actn2*) (Fig. 10). This reduction in mRNA level for *Actn2* corresponded with reduced levels of the protein in striata of BACHD mice (Fig. 11).

Importantly, decreased levels of *Actn2* are also observed in numerous models of HD and in HD patient brains (Luthi-Carter et al., 2000; Chan et al., 2002; Luthi-Carter et al., 2003; Desplats et al., 2006; Hodges et al., 2006; Becanovic et al., 2010; Thomas et al., 2011). With the addition of our study, *Actn2* down-regulation appears to be one of the most consistent transcriptional signatures of mHTT expression.

Interestingly, ACTN2 is a striatally-enriched cytoskeletal anchoring protein that is a member of the spectrin/dystrophin family of actin-bundling proteins. It is found in the post-synaptic density (PSD)-enriched synaptosomal fractions from adult rat forebrains. Additionally, it binds to NMDARs, PSD-95, CAMKIIa, and RGS9-2 and has proposed roles in the regulation of NMDA receptor localization by serving as the intermediary link between the actin cytoskeleton and NMDAR subunits, thereby influencing their clustering (Dunah et al., 2000). Importantly, depolymerization of F-actin results in the redistribution of synaptic NMDAR clusters to extra-synaptic sites (Allison et al., 1998). Furthermore, ACTN2 binding to NMDARs also alters their modulation by the calcium-binding protein calmodulin (Wyszynski et al., 1998; Dunah et al., 2000). Specifically, ACTN2 competes with calmodulin for the same binding site on NMDARs and thereby prolongs signaling through the NMDARs by preventing calmodulin-dependent inactivation of NMDARs (Wyszynski et al., 1997). Therefore, it is plausible that expression of ACTN2 in medium spiny neurons and its down-regulation in HD may contribute to mHTT-dependent dysregulation of NMDAR signaling, excitotoxicity, and the increased susceptibility of this neuronal population to pathogenic mechanisms in HD.

We directly tested the effect of ACTN2 expression on mHTT-induced toxicity, by comparing the survival of neurons expressing wild-type or mutant HTT in the presence or absence of ACTN2 in cortical primary neurons that have naturally low basal levels of ACTN2. Our results suggest an

epistatic relationship between ACTN2 and mHTT, where presence of ACTN2 is toxic to neurons expressing wt-HTT, but masks the polyQ-dependent toxicity of mHTT (Fig. 13), suggesting that mHTT and ACTN2 may be involved in similar pathways to induce neuronal death. Further studies are warranted to understand the precise nature of this relationship and may shed important insights into pathogenic mechanisms in HD.

Table 1. RNA-Seq read details.

Sample	WT STR	BACHD STR	WT CTX	BACHD CTX	WT CB	BACHD CB
Total reads	33403210	28325970	43209608	35304173	33650187	32744381
High quality (HQ) reads	31065719	26575877	40633570	33303503	31810705	30950462
HQ filtered reads (adaptor and poly A sequences removed)	31015028	26543546	40586002	33262550	31767938	30906104
HQ filtered reads (%)	92.85	93.71	93.93	94.22	94.41	94.39
unmapped left reads by TopHat (mouse)	3495836	2982541	3781661	3202563	3102707	3082338
unmapped right reads by TopHat (mouse)	3495031	2981701	3780580	3201667	3100295	3079995
unmapped paired reads by TopHat (mouse)	3495031	2981701	3780580	3201667	3100295	3079995
No. of expressed genes (by HTSeq)	21829	21347	21851	21449	21151	20914

Table 2. Striatum-enriched genes commonly dysregulated in HD brains and mouse models are not changed in the BACHD model.

Gene Symbol	Gene description	WT CB	BACHD CB	WT CTX	BACHD CTX	WT STR	BACHD STR
Drd2	Dopamine receptor D2 [Acc:MGI:94924]	12	9	210	161	1566	1519
Drd1a	Dopamine receptor D1A [Acc:MGI:99578]	6	3	352	303	1621	1680
DARPP32 (Ppp1r1b)	Protein phosphatase 1, regulatory (inhibitor) subunit 1B [Acc:MGI:94860]	1905	2011	2729	2166	12281	12068
Adora2a	Adenosine A2a receptor [Acc:MGI:99402]	21	17	286	200	2103	1894
Gpr6	G protein-coupled receptor 6 [Acc:MGI:2155249]	2	1	84	58	426	391
Pdyn	Prodynorphin [Acc:MGI:97535]	9	8	438	453	1055	1042

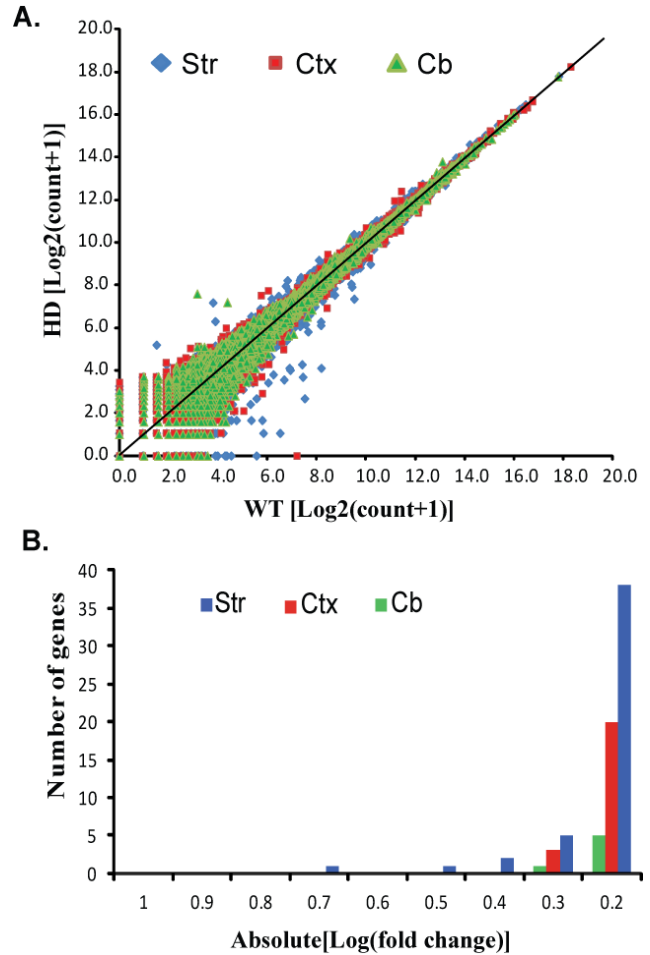
Table 3. Summary of gene expression changes between BACHD and WT littermates.

	CB	CTX	STR
Expressed* and changed >2-fold	10	21	74
Highly Expressed and changed >2-fold	0	1	5
Highly expressed and changed >25%	6	23	47

*Expressed genes were defined as those whose counts were greater than the mean of the counts for all genes in a sample.

Figure 8. Global correlation of RNA-Seq gene expression counts between BACHD and WT controls suggests few transcriptional changes in the BACHD model.

A, Expression of genes measured by RNA-Seq in BACHD and WT mice is highly concordant. Scatter plot for 8-mo brains shows the correlation in gene expression in striatum (blue), cortex (red), and cerebellum (green) of WT (x axis) vs. BACHD (y axis) mice. Each dot represents the number of sequence reads for a given gene in WT and BACHD brains transformed to log2. The black line represents a perfect correlation. Striatal (Str) Spearman correlation = 0.9825; $p < 0.0001$; Cortical (Ctx) Spearman correlation = 0.9851; $p < 0.0001$; Cerebellar (Cb) Spearman correlation = 0.9841; $p < 0.0001$. **B**, The striatum contains the most number of genes with greater than 50% change in expression (absolute[Log(fold change) > 0.2).



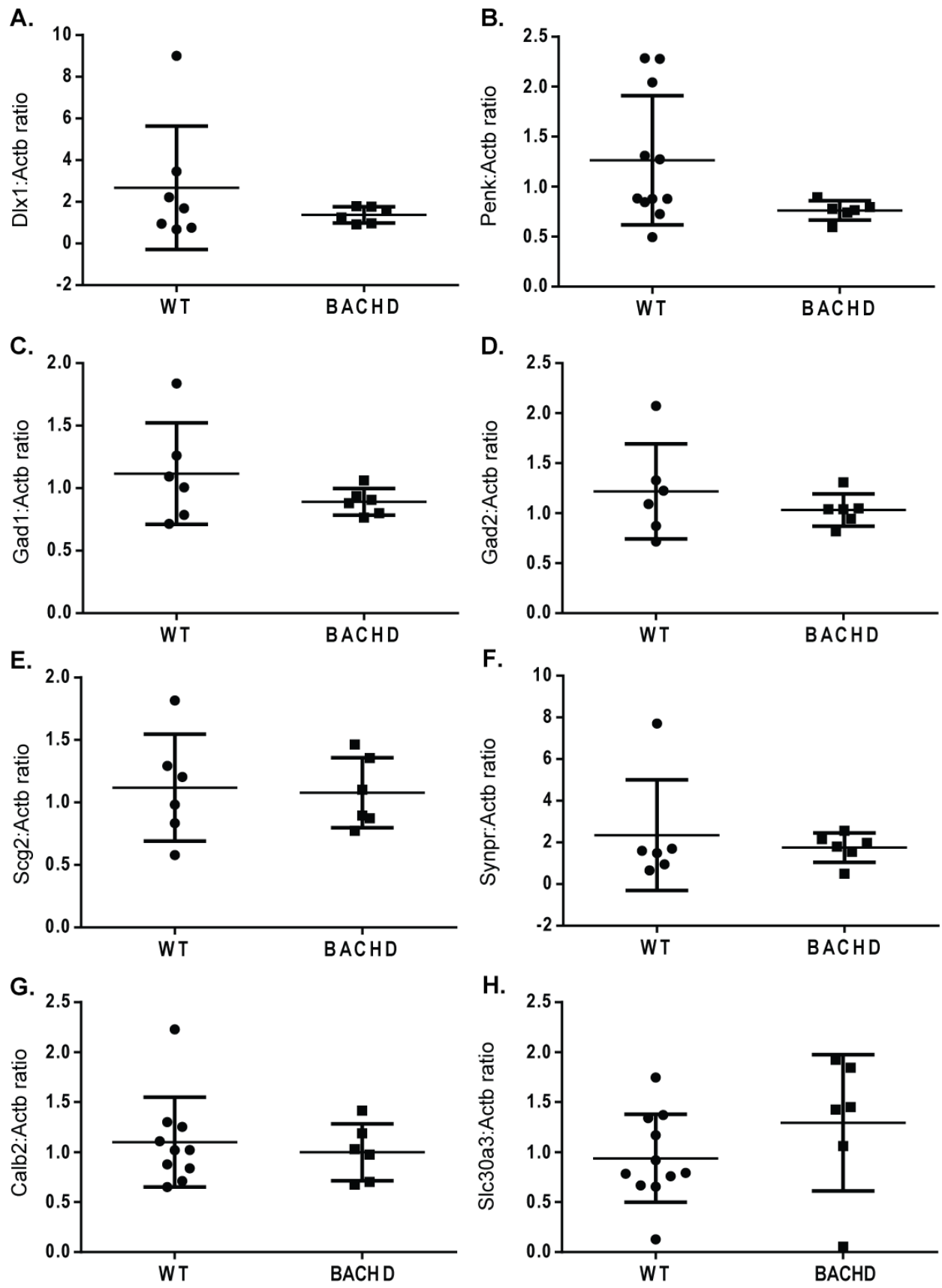
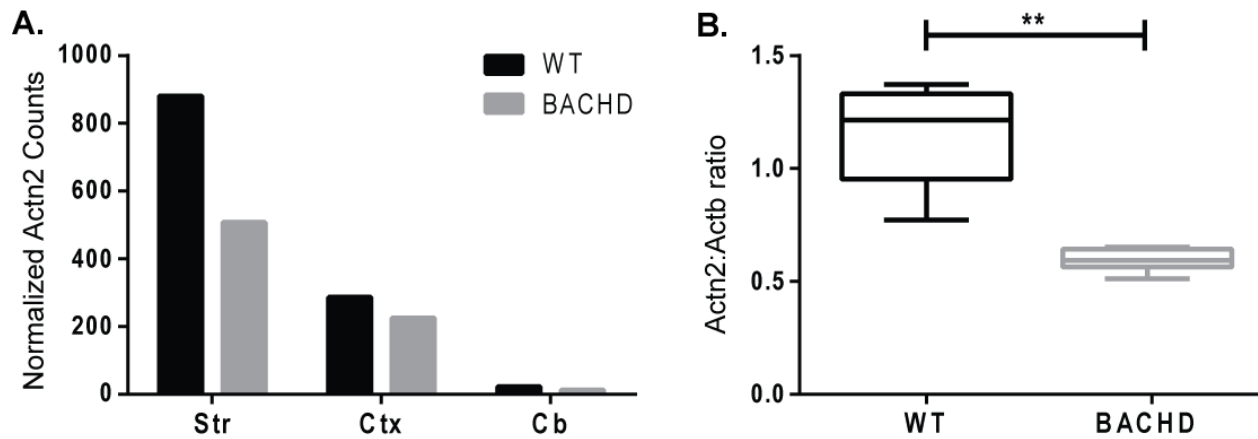


Figure 9. qRT-PCR verification of the expression of selected genes suggested by RNA-seq.

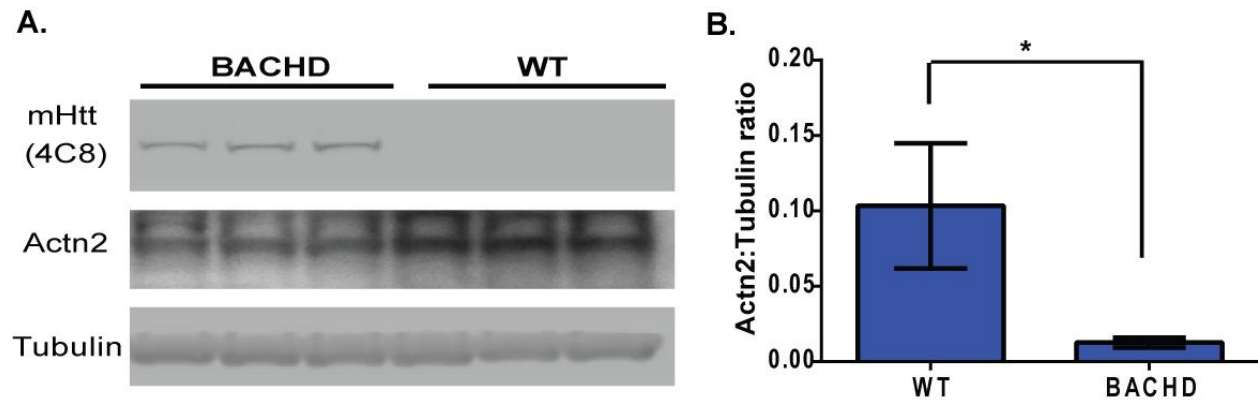
Striatal levels of distal-less homeobox 1 (*Dlx1*), pro-enkephalin (*Penk*), glutamate decarboxylase 1 (*Gad1*), glutamate decarboxylase 2 (*Gad2*), secretogranin II (*Scg2*), synaptopodin (*Synpr*), calbindin 2/calretinin (*Calb2*), and solute carrier family 30 (zinc transporter) member 3 (*Slc30a3*) mRNA are similar between BACHD and WT mice ($n = 6-11$ for WT, and 6 for BACHD). Values are based on expression levels normalized to the house-keeping gene beta-actin (*Actb*). **A**, *Dlx1*: $p = 0.3114$. **B**, *Penk*: $p = 0.0827$. **C**, *Gad1*: $p = 0.2388$. **D**, *Gad2*: $p = 0.3868$. **E**, *Scg2*: $p = 0.8504$. **F**, *Synpr*: $p = 0.6083$. **G**, *Calb2*: $p = 0.6251$. **H**, *Slc30a3*: $p = 0.2113$. Error bars represent SD.

Figure 10. *Actn2* mRNA levels are decreased in striata of BACHD mice.



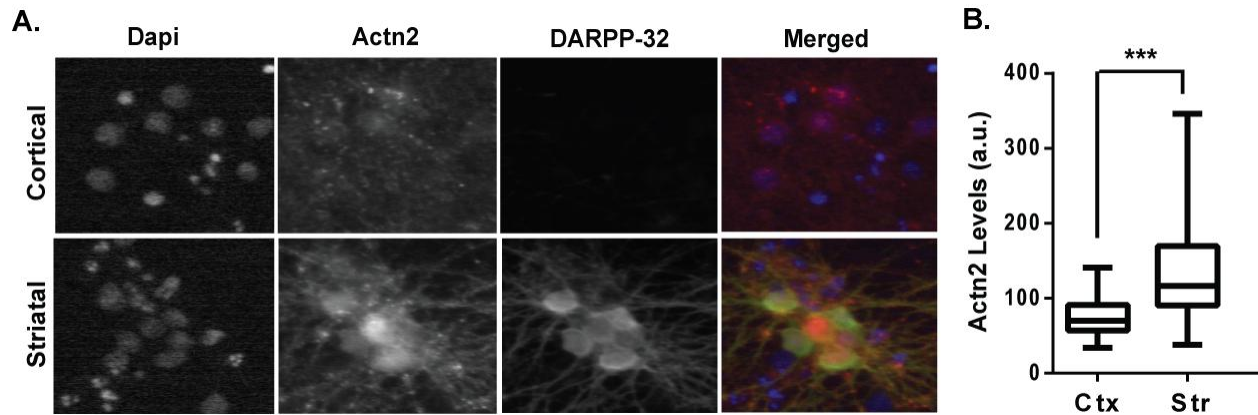
A, RNA-Seq normalized counts for *Actn2* mRNA are lower in a pooled sample of striata from three BACHD mice compared to WT controls. **B**, *Actn2* mRNA levels are also decreased by qRT-PCR in striata of BACHD mice compared to control littermates. Unpaired two-tailed Welch-corrected *t*-test with $p = 0.0014$. $N = 6$ for each genotype. $**p < 0.01$. Error bars represent SD.

Figure 11. ACTN2 protein levels are reduced in striata of BACHD mice.



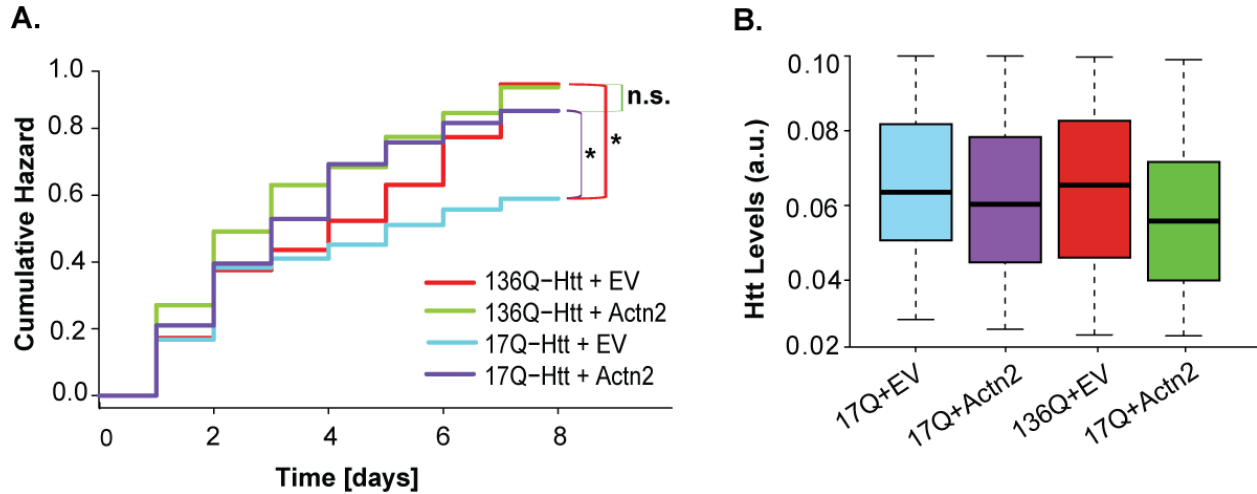
A, Representative western blot demonstrating expression level of Actn2 from striatal lysates of one-year-old BACHD and WT mice. The blot was probed with anti-expanded polyQ monoclonal antibody 4H7H7, anti-ACTN2, and anti- γ -tubulin as a loading control. **B**, Quantification of western blots demonstrating expression levels of ACTN2 from striatal lysates of one-year-old BACHD and WT mice. Values are based on the mean intensity of the ACTN2 blots with lysates from 3 mice per genotype normalized to anti- γ -tubulin control. Unpaired two-tailed t -test $p = 0.0193$. * $p < 0.01$. Error bars represent SD.

Figure 12. ACTN2 protein is highly expressed in striatal neurons.



A, Cultures of primary cortical or striatal neurons from embryonic rats were immunostained for ACTN2 and DARPP32 at 7-days *in vitro*. **B**, Quantification of Actn2 immunostaining from striatal and cortical rat cultures. Values are based on the mean fluorescent intensity of the ACTN2 staining. Unpaired two-tailed *t*-test with Welch's correction $p = 0.0001$. *** $p < 0.001$. $N = 27$ neurons for Ctx; $n = 28$ neurons for Str. Error bars represent SD.

Figure 13. ACTN2 over-expression shows an epistatic interaction with mHTT-dependent toxicity.



A, Primary cortical neurons expressing 136Q-HTT have a significantly greater cumulative risk-of-death than neurons expressing 17Q-HTT (136-HTT + EV vs. 17Q-HTT + EV: HR = 1.44; log-rank $p = 0.02417$). Expression of hACTN2 in neurons co-expressing 17Q-HTT results in a greater cumulative risk-of-death (17Q-HTT + hActn vs. 17Q-HTT + EV: HR = 1.45; log-rank $p = 0.030$), but prevents mHTT-dependent toxicity (136Q-HTT + hACTN2 vs. 17Q-HTT + hACTN2: HR = 1.105; log-rank $p = 0.425$; 136Q-HTT + hACTN2 vs. 136Q-HTT + EV: HR = 1.104; log-rank $p = 0.367$). * $p < 0.05$. **B,** Boxplot representation of HTT expression levels in neurons followed for survival in (A), 24-hrs after transfection, showing that expression levels of HTT are not different among the groups. Values are based on the mean fluorescent intensity of tagged-HTT. Expression levels of HTT are similar among all groups. N = 110 neurons for 17Q-HTT+EV; n = 297 neurons for 136Q-HTT+EV; n = 190 neurons for 17Q-HTT+hACTN2; n = 253 neurons for 136Q-HTT+hACTN2.

Chapter 4: Concluding Remarks

In this dissertation, we have described the results of our studies on the role of excitotoxicity and transcriptional dysregulation in a single mouse model of HD, namely the BACHD model developed by Gray and colleagues (Gray et al., 2008), that recapitulates key features of HD. In chapter 2, we found that deletion of the gene for the microtubule-associated protein TAU ameliorates some mHTT-dependent behavioral deficits and neuropathology *in vivo* in this HD model, suggesting that TAU plays an important role in the manifestation of these phenotypes in HD. In chapter 3, we examined the extent of transcriptional dysregulation in the BACHD model and found little evidence for large-scale perturbations in mRNA levels at an age when these mice are already symptomatic, but not exhibiting overt neurodegeneration. However, we discovered a mHTT-dependent decrease in the levels of the actin-bundling protein α -Actinin 2 (ACTN2), which mirrors observations in HD brains and virtually every other mouse model of HD that has been studied to-date. As such, *Actn2* down-regulation appears to be a core feature of HD. The specific roles that TAU and ACTN2 play in pathogenic processes mediated by mHTT are unknown and will be the subject of future work.

Interestingly, both of our studies converged on a role for cytoskeleton-associated proteins in mHTT-induced pathologies, implicating dysfunction of cytoskeletal components that influence vesicular trafficking and synaptic signaling in the disease process. Further support for a role of cytoskeletal proteins in HD pathogenesis comes from the finding that HTT-interacting proteins include several cytoskeletal associated proteins such as HIP1, tubulin, and dynactin (McMurray, 2000) and regulators of cytoskeletal and membrane dynamics such as PACSIN1 (Modregger et al., 2002; Marco et al., 2013). Furthermore, alterations of microtubule dynamics upon mHTT

expression have been reported and both microtubule stabilizing and destabilizing agents reportedly alter mHTT toxicity (Trushina et al., 2003; Varma et al., 2010).

Mutant HTT may disrupt microtubule- and actin-related process separately to cause cellular dysfunction. However, recent studies have also suggested an interplay between dynamic microtubules and the actin cytoskeleton in regulation of dendritic spine morphology and synaptic plasticity (Gu et al., 2008; Jaworski et al., 2009; Merriam et al., 2011), growth cone steering (Geraldo and Gordon-Weeks, 2009), axon branching (Dent and Kalil, 2001), and coordination of transport of membranous organelles such as lysosomes (Cordonnier et al., 2001) and the Golgi (Sahlender et al., 2005). Since some of these processes have also been implicated in the pathogenesis of HD, it is tempting to speculate that mHTT may alter association of the microtubule and actin cytoskeletons in some or all of these processes, which would tie together several distinct proposed hypotheses of pathogenic mechanisms in HD.

References

- Aarsland, D., Brønneck, K., Fladby, T., 2011. Mild cognitive impairment in Parkinson's disease. *Curr. Neurol. Neurosci. Rep.* 11, 371–378. doi:10.1007/s11910-011-0203-1
- Abada, Y.K., Schreiber, R., Ellenbroek, B., 2013. Motor, emotional and cognitive deficits in adult BACHD mice: a model for Huntington's disease. *Behav. Brain Res.* 238, 243–251. doi:10.1016/j.bbr.2012.10.039
- Allison, D.W., Gelfand, V.I., Spector, I., Craig, A.M., 1998. Role of actin in anchoring postsynaptic receptors in cultured hippocampal neurons: differential attachment of NMDA versus AMPA receptors. *J. Neurosci. Off. J. Soc. Neurosci.* 18, 2423–2436.
- Anders, S., Pyl, P.T., Huber, W., 2014. HTSeq - A Python framework to work with high-throughput sequencing data. *bioRxiv*. doi:10.1101/002824
- Andersen, P.K., Gill, R.D., 1982. Cox's Regression Model for Counting Processes: A Large Sample Study. *Ann. Stat.* 10, 1100–1120. doi:10.1214/aos/1176345976
- Anderson, S.A., Qiu, M., Bulfone, A., Eisenstat, D.D., Meneses, J., Pedersen, R., Rubenstein, J.L., 1997. Mutations of the homeobox genes *Dlx-1* and *Dlx-2* disrupt the striatal subventricular zone and differentiation of late born striatal neurons. *Neuron* 19, 27–37.
- Andrade, M.A., Petosa, C., O'Donoghue, S.I., Müller, C.W., Bork, P., 2001. Comparison of ARM and HEAT protein repeats. *J. Mol. Biol.* 309, 1–18. doi:10.1006/jmbi.2001.4624
- André, V.M., Cepeda, C., Fisher, Y.E., Huynh, M., Bardakjian, N., Singh, S., Yang, X.W., Levine, M.S., 2011. Differential Electrophysiological Changes in Striatal Output Neurons in Huntington's Disease. *J. Neurosci.* 31, 1170 –1182. doi:10.1523/JNEUROSCI.3539-10.2011

- Arrasate, M., Finkbeiner, S., 2005. Automated microscope system for determining factors that predict neuronal fate. *Proc. Natl. Acad. Sci. U. S. A.* 102, 3840–3845. doi:10.1073/pnas.0409777102
- Arrasate, M., Mitra, S., Schweitzer, E.S., Segal, M.R., Finkbeiner, S., 2004a. Inclusion body formation reduces levels of mutant huntingtin and the risk of neuronal death. *Nature* 431, 805–810. doi:10.1038/nature02998
- Arrasate, M., Mitra, S., Schweitzer, E.S., Segal, M.R., Finkbeiner, S., 2004b. Inclusion body formation reduces levels of mutant huntingtin and the risk of neuronal death. *Nature* 431, 805–810. doi:10.1038/nature02998
- Augood, S.J., Faull, R.L., Love, D.R., Emson, P.C., 1996. Reduction in enkephalin and substance P messenger RNA in the striatum of early grade Huntington's disease: a detailed cellular in situ hybridization study. *Neuroscience* 72, 1023–1036.
- Beal, M.F., Kowall, N.W., Ellison, D.W., Mazurek, M.F., Swartz, K.J., Martin, J.B., 1986. Replication of the neurochemical characteristics of Huntington's disease by quinolinic acid. *Nature* 321, 168–171. doi:10.1038/321168a0
- Becanovic, K., Pouladi, M.A., Lim, R.S., Kuhn, A., Pavlidis, P., Luthi-Carter, R., Hayden, M.R., Leavitt, B.R., 2010. Transcriptional changes in Huntington disease identified using genome-wide expression profiling and cross-platform analysis. *Hum. Mol. Genet.* 19, 1438–1452. doi:10.1093/hmg/ddq018
- Bouchard, J., Truong, J., Bouchard, K., Dunkelberger, D., Desrayaud, S., Moussaoui, S., Tabrizi, S.J., Stella, N., Muchowski, P.J., 2012. Cannabinoid Receptor 2 Signaling in Peripheral Immune Cells Modulates Disease Onset and Severity in Mouse Models of Huntington's

- Disease. *J. Neurosci. Off. J. Soc. Neurosci.* 32, 18259–18268.
doi:10.1523/JNEUROSCI.4008-12.2012
- Brooks, S.P., Dunnett, S.B., 2009. Tests to assess motor phenotype in mice: a user's guide. *Nat. Rev. Neurosci.* 10, 519–529. doi:10.1038/nrn2652
- Campean, S., Green, E.W., Breda, C., Sathyaikumar, K.V., Muchowski, P.J., Schwarcz, R., Kyriacou, C.P., Giorgini, F., 2011. The kynurenine pathway modulates neurodegeneration in a *Drosophila* model of Huntington's disease. *Curr. Biol.* CB 21, 961–966. doi:10.1016/j.cub.2011.04.028
- Caparros-Lefebvre, D., Kerdraon, O., Devos, D., Dhaenens, C.M., Blum, D., Muraige, C.A., Delacourte, A., Sablonnière, B., 2009. Association of corticobasal degeneration and Huntington's disease: can Tau aggregates protect Huntingtin toxicity? *Mov. Disord. Off. J. Mov. Disord. Soc.* 24, 1089–1090. doi:10.1002/mds.22204
- Carola, V., D'Olimpio, F., Brunamonti, E., Mangia, F., Renzi, P., 2002. Evaluation of the elevated plus-maze and open-field tests for the assessment of anxiety-related behaviour in inbred mice. *Behav. Brain Res.* 134, 49–57.
- Carroll, J.B., Southwell, A.L., Graham, R.K., Lerch, J.P., Ehrnhoefer, D.E., Cao, L.-P., Zhang, W.-N., Deng, Y., Bissada, N., Henkelman, R.M., Hayden, M.R., 2011. Mice lacking caspase-2 are protected from behavioral changes, but not pathology, in the YAC128 model of Huntington disease. *Mol. Neurodegener.* 6, 59. doi:10.1186/1750-1326-6-59
- Cepeda, C., Wu, N., André, V.M., Cummings, D.M., Levine, M.S., 2007. The corticostriatal pathway in Huntington's disease. *Prog. Neurobiol.* 81, 253–271. doi:10.1016/j.pneurobio.2006.11.001

- Cha, J.-H.J., 2000. Transcriptional dysregulation in Huntington's disease. *Trends Neurosci.* 23, 387–392. doi:10.1016/S0166-2236(00)01609-X
- Chan, E.Y.W., Luthi-Carter, R., Strand, A., Solano, S.M., Hanson, S.A., DeJohn, M.M., Kooperberg, C., Chase, K.O., DiFiglia, M., Young, A.B., Leavitt, B.R., Cha, J.-H.J., Aronin, N., Hayden, M.R., Olson, J.M., 2002. Increased huntingtin protein length reduces the number of polyglutamine-induced gene expression changes in mouse models of Huntington's disease. *Hum. Mol. Genet.* 11, 1939–1951.
- Chen, L.Y., Wei, K.-C., Huang, A.C.-Y., Wang, K., Huang, C.-Y., Yi, D., Tang, C.Y., Galas, D.J., Hood, L.E., 2012. RNASEQR—a streamlined and accurate RNA-seq sequence analysis program. *Nucleic Acids Res.* 40, e42–e42. doi:10.1093/nar/gkr1248
- Chen, N., Luo, T., Wellington, C., Metzler, M., McCutcheon, K., Hayden, M.R., Raymond, L.A., 1999. Subtype-Specific Enhancement of NMDA Receptor Currents by Mutant Huntingtin. *J. Neurochem.* 72, 1890–1898. doi:10.1111/j.1471-4159.1999.tb10200.x
- Cloud, L.J., Rosenblatt, A., Margolis, R.L., Ross, C.A., Pillai, J.A., Corey-Bloom, J., Tully, H.M., Bird, T., Panegyres, P.K., Nichter, C.A., Higgins, D.S., Helmers, S.L., Factor, S.A., Jones, R., Testa, C.M., 2012. Seizures in juvenile Huntington's disease: Frequency and characterization in a multicenter cohort. *Mov. Disord.* 27, 1797–1800. doi:10.1002/mds.25237
- Coleman, P.D., Yao, P.J., 2003. Synaptic slaughter in Alzheimer's disease. *Neurobiol. Aging* 24, 1023–1027. doi:10.1016/j.neurobiolaging.2003.09.001
- Cordonnier, M.-N., Dauzonne, D., Louvard, D., Coudrier, E., 2001. Actin Filaments and Myosin I Alpha Cooperate with Microtubules for the Movement of Lysosomes. *Mol. Biol. Cell* 12, 4013–4029. doi:10.1091/mbc.12.12.4013

- D'Souza, C.A., Chopra, V., Varhol, R., Xie, Y.-Y., Bohacec, S., Zhao, Y., Lee, L.L., Bilenky, M., Portales-Casamar, E., He, A., Wasserman, W.W., Goldowitz, D., Marra, M.A., Holt, R.A., Simpson, E.M., Jones, S.J., 2008. Identification of a set of genes showing regionally enriched expression in the mouse brain. *BMC Neurosci.* 9, 66. doi:10.1186/1471-2202-9-66
- Dau, A., Gladding, C.M., Sepers, M.D., Raymond, L.A., 2014. Chronic blockade of extrasynaptic NMDA receptors ameliorates synaptic dysfunction and pro-death signaling in Huntington disease transgenic mice. *Neurobiol. Dis.* 62, 533–542. doi:10.1016/j.nbd.2013.11.013
- Daub, A., Sharma, P., Finkbeiner, S., 2009. High-content screening of primary neurons: ready for prime time. *Curr. Opin. Neurobiol.* 19, 537–543. doi:10.1016/j.conb.2009.10.002
- Dawson, H.N., Ferreira, A., Eyster, M.V., Ghoshal, N., Binder, L.I., Vitek, M.P., 2001. Inhibition of neuronal maturation in primary hippocampal neurons from τ deficient mice. *J. Cell Sci.* 114, 1179–1187.
- Dent, E.W., Kalil, K., 2001. Axon Branching Requires Interactions between Dynamic Microtubules and Actin Filaments. *J. Neurosci.* 21, 9757–9769.
- Desplats, P.A., Kass, K.E., Gilmartin, T., Stanwood, G.D., Woodward, E.L., Head, S.R., Sutcliffe, J.G., Thomas, E.A., 2006. Selective deficits in the expression of striatal-enriched mRNAs in Huntington's disease. *J. Neurochem.* 96, 743–757. doi:10.1111/j.1471-4159.2005.03588.x
- Dong, G., Gross, K., Qiao, F., Ferguson, J., Callegari, E.A., Rezvani, K., Zhang, D., Gloeckner, C.J., Ueffing, M., Wang, H., 2012. Calretinin interacts with huntingtin and reduces

- mutant huntingtin-caused cytotoxicity. *J. Neurochem.* 123, 437–446. doi:10.1111/j.1471-4159.2012.07919.x
- Dragatsis, I., Levine, M.S., Zeitlin, S., 2000. Inactivation of *Hdh* in the brain and testis results in progressive neurodegeneration and sterility in mice. *Nat. Genet.* 26, 300–306. doi:10.1038/81593
- Dunah, A.W., Wyszynski, M., Martin, D.M., Sheng, M., Standaert, D.G., 2000. α -actinin-2 in rat striatum: localization and interaction with NMDA glutamate receptor subunits. *Brain Res. Mol. Brain Res.* 79, 77–87.
- Duyao, M.P., Auerbach, A.B., Ryan, A., Persichetti, F., Barnes, G.T., McNeil, S.M., Ge, P., Vonsattel, J.P., Gusella, J.F., Joyner, A.L., 1995. Inactivation of the mouse Huntington's disease gene homolog *Hdh*. *Science* 269, 407–410.
- Everall, I.P., DeTeresa, R., Terry, R., Masliah, E., 1997. Comparison of two quantitative methods for the evaluation of neuronal number in the frontal cortex in Alzheimer disease. *J. Neuropathol. Exp. Neurol.* 56, 1202–1206.
- Fedele, V., Roybon, L., Nordström, U., Li, J.Y., Brundin, P., 2011. Neurogenesis in the R6/2 mouse model of Huntington's disease is impaired at the level of NeuroD1. *Neuroscience* 173, 76–81. doi:10.1016/j.neuroscience.2010.08.022
- Finkbeiner, S., 2011. Huntington's Disease. *Cold Spring Harb. Perspect. Biol.* 3, a007476. doi:10.1101/cshperspect.a007476
- Geraldo, S., Gordon-Weeks, P.R., 2009. Cytoskeletal dynamics in growth-cone steering. *J. Cell Sci.* 122, 3595–3604. doi:10.1242/jcs.042309
- Gil, J.M., Rego, A.C., 2008. Mechanisms of neurodegeneration in Huntington's disease. *Eur. J. Neurosci.* 27, 2803–2820. doi:10.1111/j.1460-9568.2008.06310.x

- Goto, S., Hirano, A., 1990. Synaptophysin expression in the striatum in Huntington's disease. *Acta Neuropathol. (Berl.)* 80, 88–91.
- Gray, M., Shirasaki, D.I., Cepeda, C., Andre, V.M., Wilburn, B., Lu, X.-H., Tao, J., Yamazaki, I., Li, S.-H., Sun, Y.E., Li, X.-J., Levine, M.S., Yang, X.W., 2008. Full-Length Human Mutant Huntingtin with a Stable Polyglutamine Repeat Can Elicit Progressive and Selective Neuropathogenesis in BACHD Mice. *J Neurosci* 28, 6182–6195. doi:10.1523/JNEUROSCI.0857-08.2008
- Gu, J., Firestein, B.L., Zheng, J.Q., 2008. Microtubules in Dendritic Spine Development. *J. Neurosci.* 28, 12120–12124. doi:10.1523/JNEUROSCI.2509-08.2008
- Guidetti, P., Bates, G.P., Graham, R.K., Hayden, M.R., Leavitt, B.R., MacDonald, M.E., Slow, E.J., Wheeler, V.C., Woodman, B., Schwarcz, R., 2006. Elevated brain 3-hydroxykynurenine and quinolinate levels in Huntington disease mice. *Neurobiol. Dis.* 23, 190–197. doi:10.1016/j.nbd.2006.02.011
- Hansson, O., Guatteo, E., Mercuri, N.B., Bernardi, G., Li, X.J., Castilho, R.F., Brundin, P., 2001. Resistance to NMDA toxicity correlates with appearance of nuclear inclusions, behavioural deficits and changes in calcium homeostasis in mice transgenic for exon 1 of the huntington gene. *Eur. J. Neurosci.* 14, 1492–1504.
- Harjes, P., Wanker, E.E., 2003. The hunt for huntingtin function: interaction partners tell many different stories. *Trends Biochem. Sci.* 28, 425–433. doi:10.1016/S0968-0004(03)00168-3
- Hassel, B., Tessler, S., Faull, R.L.M., Emson, P.C., 2008. Glutamate uptake is reduced in prefrontal cortex in Huntington's disease. *Neurochem. Res.* 33, 232–237. doi:10.1007/s11064-007-9463-1

- Heng, M.Y., Detloff, P.J., Wang, P.L., Tsien, J.Z., Albin, R.L., 2009. In Vivo Evidence for NMDA Receptor-Mediated Excitotoxicity in a Murine Genetic Model of Huntington Disease. *J Neurosci* 29, 3200–3205. doi:10.1523/JNEUROSCI.5599-08.2009
- Hodges, A., Strand, A.D., Aragaki, A.K., Kuhn, A., Sengstag, T., Hughes, G., Elliston, L.A., Hartog, C., Goldstein, D.R., Thu, D., Hollingsworth, Z.R., Collin, F., Synek, B., Holmans, P.A., Young, A.B., Wexler, N.S., Delorenzi, M., Kooperberg, C., Augood, S.J., Faull, R.L.M., Olson, J.M., Jones, L., Luthi-Carter, R., 2006. Regional and cellular gene expression changes in human Huntington's disease brain. *Hum. Mol. Genet.* 15, 965–977. doi:10.1093/hmg/ddl013
- Hosmer, D.W., Lemeshow, S., 1999. *Applied Survival Analysis: Regression Modeling of Time to Event Data*. John Wiley & Sons, Inc.
- Ide, K., Nukina, N., Masuda, N., Goto, J., Kanazawa, I., 1995. Abnormal gene product identified in Huntington's disease lymphocytes and brain. *Biochem. Biophys. Res. Commun.* 209, 1119–1125. doi:10.1006/bbrc.1995.1613
- Ittner, L.M., Ke, Y.D., Delerue, F., Bi, M., Gladbach, A., van Eersel, J., Wölfing, H., Chieng, B.C., Christie, M.J., Napier, I.A., Eckert, A., Staufenbiel, M., Hardeman, E., Götz, J., 2010. Dendritic Function of Tau Mediates Amyloid- β Toxicity in Alzheimer's Disease Mouse Models. *Cell* 142, 387–397. doi:10.1016/j.cell.2010.06.036
- Jaffar, S., Counts, S.E., Ma, S.Y., Dadko, E., Gordon, M.N., Morgan, D., Mufson, E.J., 2001. Neuropathology of mice carrying mutant APP(swe) and/or PS1(M146L) transgenes: alterations in the p75(NTR) cholinergic basal forebrain septohippocampal pathway. *Exp. Neurol.* 170, 227–243. doi:10.1006/exnr.2001.7710

- Jager, K.J., van Dijk, P.C., Zoccali, C., Dekker, F.W., 2008. The analysis of survival data: the Kaplan-Meier method. *Kidney Int.* 74, 560–565. doi:10.1038/ki.2008.217
- Jaworski, J., Kapitein, L.C., Gouveia, S.M., Dortland, B.R., Wulf, P.S., Grigoriev, I., Camera, P., Spangler, S.A., Di Stefano, P., Demmers, J., Krugers, H., Defilippi, P., Akhmanova, A., Hoogenraad, C.C., 2009. Dynamic Microtubules Regulate Dendritic Spine Morphology and Synaptic Plasticity. *Neuron* 61, 85–100. doi:10.1016/j.neuron.2008.11.013
- Jia, H., Kast, R.J., Steffan, J.S., Thomas, E.A., 2012. Selective histone deacetylase (HDAC) inhibition imparts beneficial effects in Huntington’s disease mice: implications for the ubiquitin–proteasomal and autophagy systems. *Hum. Mol. Genet.* 21, 5280–5293. doi:10.1093/hmg/dds379
- Joshi, P.R., Wu, N.-P., André, V.M., Cummings, D.M., Cepeda, C., Joyce, J.A., Carroll, J.B., Leavitt, B.R., Hayden, M.R., Levine, M.S., Bamford, N.S., 2009. Age-dependent alterations of corticostriatal activity in the YAC128 mouse model of Huntington disease. *J. Neurosci. Off. J. Soc. Neurosci.* 29, 2414–2427. doi:10.1523/JNEUROSCI.5687-08.2009
- Kaltenbach, L.S., Romero, E., Becklin, R.R., Chettier, R., Bell, R., Phansalkar, A., Strand, A., Torcassi, C., Savage, J., Hurlburt, A., Cha, G.-H., Ukani, L., Chepanoske, C.L., Zhen, Y., Sahasrabudhe, S., Olson, J., Kurschner, C., Ellerby, L.M., Peltier, J.M., Botas, J., Hughes, R.E., 2007. Huntingtin interacting proteins are genetic modifiers of neurodegeneration. *PLoS Genet.* 3, e82. doi:10.1371/journal.pgen.0030082
- Kremer, B., Clark, C.M., Almqvist, E.W., Raymond, L.A., Graf, P., Jacova, C., Mezei, M., Hardy, M.A., Snow, B., Martin, W., Hayden, M.R., 1999. Influence of lamotrigine on

- progression of early Huntington disease: a randomized clinical trial. *Neurology* 53, 1000–1011.
- Kuhn, A., Goldstein, D.R., Hodges, A., Strand, A.D., Sengstag, T., Kooperberg, C., Becanovic, K., Pouladi, M.A., Sathasivam, K., Cha, J.-H.J., Hannan, A.J., Hayden, M.R., Leavitt, B.R., Dunnett, S.B., Ferrante, R.J., Albin, R., Shelbourne, P., Delorenzi, M., Augood, S.J., Faull, R.L.M., Olson, J.M., Bates, G.P., Jones, L., Luthi-Carter, R., 2007. Mutant huntingtin's effects on striatal gene expression in mice recapitulate changes observed in human Huntington's disease brain and do not differ with mutant huntingtin length or wild-type huntingtin dosage. *Hum. Mol. Genet.* 16, 1845–1861. doi:10.1093/hmg/ddm133
- Kwan, W., Magnusson, A., Chou, A., Adame, A., Carson, M.J., Kohsaka, S., Masliah, E., Moller, T., Ransohoff, R., Tabrizi, S.J., Bjorkqvist, M., Muchowski, P.J., 2012. Bone Marrow Transplantation Confers Modest Benefits in Mouse Models of Huntington's Disease. *J. Neurosci. Off. J. Soc. Neurosci.* 32, 133–142. doi:10.1523/JNEUROSCI.4846-11.2012
- Landwehrmeyer, G.B., Dubois, B., de Yébenes, J.G., Kremer, B., Gaus, W., Kraus, P.H., Przuntek, H., Dib, M., Doble, A., Fischer, W., Ludolph, A.C., 2007. Riluzole in Huntington's disease: a 3-year, randomized controlled study. *Ann. Neurol.* 62, 262–272. doi:10.1002/ana.21181
- Levine, M.S., Klapstein, G.J., Koppel, A., Gruen, E., Cepeda, C., Vargas, M.E., Jokel, E.S., Carpenter, E.M., Zanjani, H., Hurst, R.S., Efstratiadis, A., Zeitlin, S., Chesselet, M.F., 1999. Enhanced sensitivity to N-methyl-D-aspartate receptor activation in transgenic and knockin mouse models of Huntington's disease. *J. Neurosci. Res.* 58, 515–532.

- Li, L., Fan, M., Icton, C.D., Chen, N., Leavitt, B.R., Hayden, M.R., Murphy, T.H., Raymond, L.A., 2003. Role of NR2B-type NMDA receptors in selective neurodegeneration in Huntington disease. *Neurobiol. Aging* 24, 1113–1121.
- Li, S.-H., Li, X.-J., 2004. Huntingtin–protein interactions and the pathogenesis of Huntington’s disease. *Trends Genet.* 20, 146–154. doi:10.1016/j.tig.2004.01.008
- Li, S.-H., Schilling, G., Young, W.S., Li, X.-., Margolis, R.L., Stine, O.C., Wagster, M.V., Abbott, M.H., Franz, M.L., Ranen, N.G., Folstein, S.E., Hedreen, J.C., Ross, C.A., 1993. Huntington’s disease gene (IT15) is widely expressed in human and rat tissues. *Neuron* 11, 985–993. doi:10.1016/0896-6273(93)90127-D
- Liévens, J.C., Woodman, B., Mahal, A., Spasic-Bosovic, O., Samuel, D., Kerkerian-Le Goff, L., Bates, G.P., 2001. Impaired glutamate uptake in the R6 Huntington’s disease transgenic mice. *Neurobiol. Dis.* 8, 807–821. doi:10.1006/nbdi.2001.0430
- Lipinski, M.M., Yuan, J., 2004. Mechanisms of cell death in polyglutamine expansion diseases. *Curr. Opin. Pharmacol.* 4, 85–90. doi:10.1016/j.coph.2003.09.008
- Liu, Y., Lv, K., Li, Z., Yu, A.C.H., Chen, J., Teng, J., 2012. PACSIN1, a Tau-interacting Protein, Regulates Axonal Elongation and Branching by Facilitating Microtubule Instability. *J. Biol. Chem.* 287, 39911–39924. doi:10.1074/jbc.M112.403451
- Lundh, S.H., Nilsson, N., Soylu, R., Kirik, D., Petersén, Å., 2013. Hypothalamic expression of mutant huntingtin contributes to the development of depressive-like behavior in the BAC transgenic mouse model of Huntington’s disease. *Hum. Mol. Genet.* 22, 3485–3497. doi:10.1093/hmg/ddt203

- Lundh, S.H., Soyulu, R., Petersen, A., 2012. Expression of Mutant Huntingtin in Leptin Receptor-Expressing Neurons Does Not Control the Metabolic and Psychiatric Phenotype of the BACHD Mouse. *PLoS ONE* 7. doi:10.1371/journal.pone.0051168
- Luthi-Carter, R., Apostol, B.L., Dunah, A.W., DeJohn, M.M., Farrell, L.A., Bates, G.P., Young, A.B., Standaert, D.G., Thompson, L.M., Cha, J.-H.J., 2003. Complex alteration of NMDA receptors in transgenic Huntington's disease mouse brain: analysis of mRNA and protein expression, plasma membrane association, interacting proteins, and phosphorylation. *Neurobiol. Dis.* 14, 624–636. doi:10.1016/j.nbd.2003.08.024
- Luthi-Carter, R., Hanson, S.A., Strand, A.D., Bergstrom, D.A., Chun, W., Peters, N.L., Woods, A.M., Chan, E.Y., Kooperberg, C., Krainc, D., Young, A.B., Tapscott, S.J., Olson, J.M., 2002. Dysregulation of gene expression in the R6/2 model of polyglutamine disease: parallel changes in muscle and brain. *Hum. Mol. Genet.* 11, 1911–1926. doi:10.1093/hmg/11.17.1911
- Luthi-Carter, R., Strand, A., Peters, N.L., Solano, S.M., Hollingsworth, Z.R., Menon, A.S., Frey, A.S., Spektor, B.S., Penney, E.B., Schilling, G., Ross, C.A., Borchelt, D.R., Tapscott, S.J., Young, A.B., Cha, J.-H.J., Olson, J.M., 2000. Decreased expression of striatal signaling genes in a mouse model of Huntington's disease. *Hum. Mol. Genet.* 9, 1259–1271. doi:10.1093/hmg/9.9.1259
- Marco, S., Giralt, A., Petrovic, M.M., Pouladi, M.A., Martínez-Turrillas, R., Martínez-Hernández, J., Kaltenbach, L.S., Torres-Peraza, J., Graham, R.K., Watanabe, M., Luján, R., Nakanishi, N., Lipton, S.A., Lo, D.C., Hayden, M.R., Alberch, J., Wesseling, J.F., Pérez-Otaño, I., 2013. Suppressing aberrant GluN3A expression rescues synaptic and

- behavioral impairments in Huntington's disease models. *Nat. Med.* 19, 1030–1038.
doi:10.1038/nm.3246
- Massouh, M., Wallman, M.-J., Pourcher, E., Parent, A., 2008. The fate of the large striatal interneurons expressing calretinin in Huntington's disease. *Neurosci. Res.* 62, 216–224.
doi:10.1016/j.neures.2008.08.007
- Mazarei, G., Neal, S.J., Becanovic, K., Luthi-Carter, R., Simpson, E.M., Leavitt, B.R., 2009. Expression analysis of novel striatal-enriched genes in Huntington disease. *Hum Mol Genet* ddp527. doi:10.1093/hmg/ddp527
- McGeer, E.G., McGeer, P.L., 1976. Duplication of biochemical changes of Huntington's chorea by intrastriatal injections of glutamic and kainic acids. *Nature* 263, 517–519.
- McMurray, C.T., 2000. Neurodegeneration: diseases of the cytoskeleton? *Publ. Online* 28 Sept. 2000 Doi101038sjcdd4400764 7. doi:10.1038/sj.cdd.4400764
- Menalled, L., El-Khodori, B.F., Patry, M., Suárez-Fariñas, M., Orenstein, S.J., Zahasky, B., Leahy, C., Wheeler, V., Yang, X.W., MacDonald, M., Morton, A.J., Bates, G., Leeds, J., Park, L., Howland, D., Signer, E., Tobin, A., Brunner, D., 2009. Systematic behavioral evaluation of Huntington's disease transgenic and knock-in mouse models. *Neurobiol. Dis.* 35, 319–336. doi:10.1016/j.nbd.2009.05.007
- Merriam, E.B., Lombard, D.C., Viesselmann, C., Ballweg, J., Stevenson, M., Pietila, L., Hu, X., Dent, E.W., 2011. Dynamic Microtubules Promote Synaptic NMDA Receptor-Dependent Spine Enlargement. *PLoS ONE* 6, e27688. doi:10.1371/journal.pone.0027688
- Metzler, M., Gan, L., Pan Wong, T., Liu, L., Helm, J., Liu, L., Georgiou, J., Wang, Y., Bissada, N., Cheng, K., Roder, J.C., Wang, Y.T., Hayden, M.R., 2007. NMDA Receptor Function and NMDA Receptor-Dependent Phosphorylation of Huntingtin Is Altered by the

- Endocytic Protein HIP1. *J Neurosci* 27, 2298–2308. doi:10.1523/JNEUROSCI.5175-06.2007
- Miller, B.R., Dorner, J.L., Shou, M., Sari, Y., Barton, S.J., Sengelaub, D.R., Kennedy, R.T., Rebec, G.V., 2008. Up-regulation of GLT1 expression increases glutamate uptake and attenuates the Huntington's disease phenotype in the R6/2 mouse. *Neuroscience* 153, 329–337. doi:10.1016/j.neuroscience.2008.02.004
- Miller, J., Arrasate, M., Brooks, E., Peters-Libeu, C., Legleiter, J., Hatters, D., Curtis, J., Cheung, K., Krishnan, P., Mitra, S., Widjaja, K., Shaby, B.A., Lotz, G.P., Newhouse, Y., Mitchell, E., Osmand, A., Gray, M., Thulasiramin, V., Saudou, F., Segal, M., Yang, X.W., Masliah, E., Thompson, L.M., Muchowski, P.J., Weisgraber, K.H., Finkbeiner, S., 2011. Identifying polyglutamine protein species in situ that best predict neurodegeneration. *Nat. Chem. Biol.* 7, 925–934. doi:10.1038/nchembio.694
- Miller, J., Arrasate, M., Shaby, B.A., Mitra, S., Masliah, E., Finkbeiner, S., 2010. Quantitative Relationships between Huntingtin Levels, Polyglutamine Length, Inclusion Body Formation, and Neuronal Death Provide Novel Insight into Huntington's Disease Molecular Pathogenesis. *J. Neurosci.* 30, 10541–10550. doi:10.1523/JNEUROSCI.0146-10.2010
- Modregger, J., DiProspero, N.A., Charles, V., Tagle, D.A., Plomann, M., 2002. PACSIN 1 interacts with huntingtin and is absent from synaptic varicosities in presymptomatic Huntington's disease brains. *Hum. Mol. Genet.* 11, 2547–2558.
- Morris, M., Koyama, A., Masliah, E., Mucke, L., 2011a. Tau Reduction Does Not Prevent Motor Deficits in Two Mouse Models of Parkinson's Disease. *PLoS ONE* 6, e29257. doi:10.1371/journal.pone.0029257

- Morris, M., Maeda, S., Vossel, K., Mucke, L., 2011b. The Many Faces of Tau. *Neuron* 70, 410–426. doi:10.1016/j.neuron.2011.04.009
- Nasir, J., Floresco, S.B., O’Kusky, J.R., Diewert, V.M., Richman, J.M., Zeisler, J., Borowski, A., Marth, J.D., Phillips, A.G., Hayden, M.R., 1995. Targeted disruption of the Huntington’s disease gene results in embryonic lethality and behavioral and morphological changes in heterozygotes. *Cell* 81, 811–823.
- Nguyen, H.P., Kobbe, P., Rahne, H., Wörpel, T., Jäger, B., Stephan, M., Pabst, R., Holzmann, C., Riess, O., Korr, H., Kántor, O., Petrasch-Parwez, E., Wetzel, R., Osmand, A., von Hörsten, S., 2006. Behavioral abnormalities precede neuropathological markers in rats transgenic for Huntington’s disease. *Hum. Mol. Genet.* 15, 3177–3194. doi:10.1093/hmg/ddl394
- Okamoto, S., Pouladi, M.A., Talantova, M., Yao, D., Xia, P., Ehrnhoefer, D.E., Zaidi, R., Clemente, A., Kaul, M., Graham, R.K., Zhang, D., Vincent Chen, H.-S., Tong, G., Hayden, M.R., Lipton, S.A., 2009. Balance between synaptic versus extrasynaptic NMDA receptor activity influences inclusions and neurotoxicity of mutant huntingtin. *Nat Med* 15, 1407–1413. doi:10.1038/nm.2056
- Orr, A.L., Li, S., Wang, C.-E., Li, H., Wang, J., Rong, J., Xu, X., Mastroberardino, P.G., Greenamyre, J.T., Li, X.-J., 2008. N-Terminal Mutant Huntingtin Associates with Mitochondria and Impairs Mitochondrial Trafficking. *J Neurosci* 28, 2783–2792. doi:10.1523/JNEUROSCI.0106-08.2008
- Pacheco, C.D., Elrick, M.J., Lieberman, A.P., 2009. Tau deletion exacerbates the phenotype of Niemann–Pick type C mice and implicates autophagy in pathogenesis. *Hum. Mol. Genet.* 18, 956–965. doi:10.1093/hmg/ddn423

- Palop, J.J., Chin, J., Roberson, E.D., Wang, J., Thwin, M.T., Bien-Ly, N., Yoo, J., Ho, K.O., Yu, G.-Q., Kreitzer, A., Finkbeiner, S., Noebels, J.L., Mucke, L., 2007. Aberrant excitatory neuronal activity and compensatory remodeling of inhibitory hippocampal circuits in mouse models of Alzheimer's disease. *Neuron* 55, 697–711. doi:10.1016/j.neuron.2007.07.025
- Palop, J.J., Mucke, L., Roberson, E.D., 2011. Quantifying biomarkers of cognitive dysfunction and neuronal network hyperexcitability in mouse models of Alzheimer's disease: depletion of calcium-dependent proteins and inhibitory hippocampal remodeling. *Methods Mol. Biol. Clifton NJ* 670, 245–262. doi:10.1007/978-1-60761-744-0_17
- Paulsen, J.S., Langbehn, D.R., Stout, J.C., Aylward, E., Ross, C.A., Nance, M., Guttman, M., Johnson, S., MacDonald, M., Beglinger, L.J., Duff, K., Kayson, E., Biglan, K., Shoulson, I., Oakes, D., Hayden, M., 2008. Detection of Huntington's disease decades before diagnosis: the Predict-HD study. *J. Neurol. Neurosurg. Psychiatry* 79, 874–880. doi:10.1136/jnnp.2007.128728
- Paulsen, J.S., Ready, R.E., Hamilton, J.M., Mega, M.S., Cummings, J.L., 2001. Neuropsychiatric aspects of Huntington's disease. *J. Neurol. Neurosurg. Psychiatry* 71, 310–314.
- Perutz, M.F., Windle, A.H., 2001. Cause of neural death in neurodegenerative diseases attributable to expansion of glutamine repeats. *Nature* 412, 143–144. doi:10.1038/35084141
- Pouladi, M.A., Graham, R.K., Karasinska, J.M., Xie, Y., Santos, R.D., Petersén, A., Hayden, M.R., 2009. Prevention of depressive behaviour in the YAC128 mouse model of Huntington disease by mutation at residue 586 of huntingtin. *Brain J. Neurol.* 132, 919–932. doi:10.1093/brain/awp006

- Pouladi, M.A., Morton, A.J., Hayden, M.R., 2013. Choosing an animal model for the study of Huntington's disease. *Nat. Rev. Neurosci.* 14, 708–721. doi:10.1038/nrn3570
- Pouladi, M.A., Stanek, L.M., Xie, Y., Franciosi, S., Southwell, A.L., Deng, Y., Butland, S., Zhang, W., Cheng, S.H., Shihabuddin, L.S., Hayden, M.R., 2012. Marked differences in neurochemistry and aggregates despite similar behavioural and neuropathological features of Huntington disease in the full-length BACHD and YAC128 mice. *Hum. Mol. Genet.* 21, 2219–2232. doi:10.1093/hmg/dds037
- Raymond, L.A., André, V.M., Cepeda, C., Gladding, C.M., Milnerwood, A.J., Levine, M.S., 2011. Pathophysiology of Huntington's disease: time-dependent alterations in synaptic and receptor function. *Neuroscience* 198, 252–273. doi:10.1016/j.neuroscience.2011.08.052
- Richfield, E.K., Maguire-Zeiss, K.A., Cox, C., Gilmore, J., Voorn, P., 1995. Reduced expression of preproenkephalin in striatal neurons from Huntington's disease patients. *Ann. Neurol.* 37, 335–343. doi:10.1002/ana.410370309
- Roberson, E.D., Halabisky, B., Yoo, J.W., Yao, J., Chin, J., Yan, F., Wu, T., Hamto, P., Devidze, N., Yu, G.-Q., Palop, J.J., Noebels, J.L., Mucke, L., 2011. Amyloid- β /Fyn-induced synaptic, network, and cognitive impairments depend on tau levels in multiple mouse models of Alzheimer's disease. *J. Neurosci. Off. J. Soc. Neurosci.* 31, 700–711. doi:10.1523/JNEUROSCI.4152-10.2011
- Roberson, E.D., Scarce-Lavie, K., Palop, J.J., Yan, F., Cheng, I.H., Wu, T., Gerstein, H., Yu, G.-Q., Mucke, L., 2007. Reducing Endogenous Tau Ameliorates Amyloid {beta}-Induced Deficits in an Alzheimer's Disease Mouse Model. *Science* 316, 750–754. doi:10.1126/science.1141736

- Rosas, H.D., Liu, A.K., Hersch, S., Glessner, M., Ferrante, R.J., Salat, D.H., Kouwe, A. van der, Jenkins, B.G., Dale, A.M., Fischl, B., 2002. Regional and progressive thinning of the cortical ribbon in Huntington's disease. *Neurology* 58, 695–701. doi:10.1212/WNL.58.5.695
- Rosen, G.D., Williams, R.W., 2001. Complex trait analysis of the mouse striatum: independent QTLs modulate volume and neuron number. *BMC Neurosci.* 2, 5. doi:10.1186/1471-2202-2-5
- Ross, C.A., 1995. When more is less: Pathogenesis of glutamine repeat neurodegenerative diseases. *Neuron* 15, 493–496. doi:10.1016/0896-6273(95)90138-8
- Roze, E., Saudou, F., Caboche, J., 2008. Pathophysiology of Huntington's disease: from huntingtin functions to potential treatments. *Curr. Opin. Neurol.* 21, 497–503. doi:10.1097/WCO.0b013e328304b692
- Runne, H., Régulier, E., Kuhn, A., Zala, D., Gokce, O., Perrin, V., Sick, B., Aebischer, P., Déglon, N., Luthi-Carter, R., 2008. Dysregulation of gene expression in primary neuron models of Huntington's disease shows that polyglutamine-related effects on the striatal transcriptome may not be dependent on brain circuitry. *J. Neurosci. Off. J. Soc. Neurosci.* 28, 9723–9731. doi:10.1523/JNEUROSCI.3044-08.2008
- Sahlender, D.A., Roberts, R.C., Arden, S.D., Spudich, G., Taylor, M.J., Luzio, J.P., Kendrick-Jones, J., Buss, F., 2005. Optineurin links myosin VI to the Golgi complex and is involved in Golgi organization and exocytosis. *J. Cell Biol.* 169, 285–295. doi:10.1083/jcb.200501162

- Samuels, B.A., Hen, R., 2011. Novelty-Suppressed Feeding in the Mouse, in: Gould, T.D. (Ed.), Mood and Anxiety Related Phenotypes in Mice, *Neuromethods*. Humana Press, pp. 107–121.
- Sanchez, P.E., Zhu, L., Verret, L., Vossel, K.A., Orr, A.G., Cirrito, J.R., Devidze, N., Ho, K., Yu, G.-Q., Palop, J.J., Mucke, L., 2012. Levetiracetam suppresses neuronal network dysfunction and reverses synaptic and cognitive deficits in an Alzheimer’s disease model. *Proc. Natl. Acad. Sci. U. S. A.* 109, E2895–2903. doi:10.1073/pnas.1121081109
- Sapp, E., Ge, P., Aizawa, H., Bird, E., Penney, J., Young, A.B., Vonsattel, J.P., DiFiglia, M., 1995. Evidence for a preferential loss of enkephalin immunoreactivity in the external globus pallidus in low grade Huntington’s disease using high resolution image analysis. *Neuroscience* 64, 397–404.
- Saudou, F., Finkbeiner, S., Devys, D., Greenberg, M.E., 1998. Huntingtin acts in the nucleus to induce apoptosis but death does not correlate with the formation of intranuclear inclusions. *Cell* 95, 55–66.
- Schulte, J., Littleton, J.T., 2011. The biological function of the Huntingtin protein and its relevance to Huntington’s Disease pathology. *Curr. Trends Neurol.* 5, 65–78.
- Seredenina, T., Luthi-Carter, R., 2012. What have we learned from gene expression profiles in Huntington’s disease? *Neurobiol. Dis.* 45, 83–98. doi:10.1016/j.nbd.2011.07.001
- Shirasaki, D.I., Greiner, E.R., Al-Ramahi, I., Gray, M., Boontheung, P., Geschwind, D.H., Botas, J., Coppola, G., Horvath, S., Loo, J.A., Yang, X.W., 2012. Network organization of the huntingtin proteomic interactome in mammalian brain. *Neuron* 75, 41–57. doi:10.1016/j.neuron.2012.05.024

- Shirendeb, U.P., Calkins, M.J., Manczak, M., Anekonda, V., Dufour, B., McBride, J.L., Mao, P., Reddy, P.H., 2012. Mutant huntingtin's interaction with mitochondrial protein Drp1 impairs mitochondrial biogenesis and causes defective axonal transport and synaptic degeneration in Huntington's disease. *Hum. Mol. Genet.* 21, 406–420. doi:10.1093/hmg/ddr475
- Sipione, S., Rigamonti, D., Valenza, M., Zuccato, C., Conti, L., Pritchard, J., Kooperberg, C., Olson, J.M., Cattaneo, E., 2002. Early transcriptional profiles in huntingtin-inducible striatal cells by microarray analyses. *Hum. Mol. Genet.* 11, 1953–1965.
- Slow, E.J., Graham, R.K., Osmand, A.P., Devon, R.S., Lu, G., Deng, Y., Pearson, J., Vaid, K., Bissada, N., Wetzel, R., Leavitt, B.R., Hayden, M.R., 2005. Absence of behavioral abnormalities and neurodegeneration in vivo despite widespread neuronal huntingtin inclusions. *Proc. Natl. Acad. Sci. U. S. A.* 102, 11402–11407. doi:10.1073/pnas.0503634102
- Smith, R., Bacos, K., Fedele, V., Soulet, D., Walz, H.A., Obermüller, S., Lindqvist, A., Björkqvist, M., Klein, P., Onnerfjord, P., Brundin, P., Mulder, H., Li, J.-Y., 2009. Mutant huntingtin interacts with β -tubulin and disrupts vesicular transport and insulin secretion. *Hum. Mol. Genet.* 18, 3942–3954. doi:10.1093/hmg/ddp336
- Sonmez, O.F., Odaci, E., Bas, O., Colakoglu, S., Sahin, B., Bilgic, S., Kaplan, S., 2010. A stereological study of MRI and the Cavalieri principle combined for diagnosis and monitoring of brain tumor volume. *J. Clin. Neurosci. Off. J. Neurosurg. Soc. Australas.* 17, 1499–1502. doi:10.1016/j.jocn.2010.03.044

- Spampanato, J., Gu, X., Yang, X.W., Mody, I., 2008. Progressive synaptic pathology of motor cortical neurons in a BAC transgenic mouse model of Huntington's disease. *Neuroscience* 157, 606–620. doi:10.1016/j.neuroscience.2008.09.020
- Spillantini, M.G., Goedert, M., 2013. Tau pathology and neurodegeneration. *Lancet Neurol.* 12, 609–622. doi:10.1016/S1474-4422(13)70090-5
- Steffan, J.S., Bodai, L., Pallos, J., Poelman, M., McCampbell, A., Apostol, B.L., Kazantsev, A., Schmidt, E., Zhu, Y.Z., Greenwald, M., Kurokawa, R., Housman, D.E., Jackson, G.R., Marsh, J.L., Thompson, L.M., 2001. Histone deacetylase inhibitors arrest polyglutamine-dependent neurodegeneration in *Drosophila*. *Nature* 413, 739–743. doi:10.1038/35099568
- Strong, T.V., Tagle, D.A., Valdes, J.M., Elmer, L.W., Boehm, K., Swaroop, M., Kaatz, K.W., Collins, F.S., Albin, R.L., 1993. Widespread expression of the human and rat Huntington's disease gene in brain and nonneural tissues. *Nat Genet* 5, 259–265. doi:10.1038/ng1193-259
- Sugars, K.L., Rubinsztein, D.C., 2003. Transcriptional abnormalities in Huntington disease. *Trends Genet.* 19, 233–238. doi:10.1016/S0168-9525(03)00074-X
- Sun, Y., Savanenin, A., Reddy, P.H., Liu, Y.F., 2001. Polyglutamine-expanded huntingtin promotes sensitization of N-methyl-D-aspartate receptors via post-synaptic density 95. *J. Biol. Chem.* 276, 24713–24718. doi:10.1074/jbc.M103501200
- Tallaksen-Greene, S.J., Janiszewska, A., Benton, K., Ruprecht, L., Albin, R.L., 2010. Lack of efficacy of NMDA receptor-NR2B selective antagonists in the R6/2 model of Huntington disease. *Exp. Neurol.* 225, 402–407. doi:10.1016/j.expneurol.2010.07.015

- Tang, T.-S., Slow, E., Lupu, V., Stavrovskaya, I.G., Sugimori, M., Llinás, R., Kristal, B.S., Hayden, M.R., Bezprozvanny, I., 2005. Disturbed Ca²⁺ signaling and apoptosis of medium spiny neurons in Huntington's disease. *Proc. Natl. Acad. Sci. U. S. A.* 102, 2602–2607. doi:10.1073/pnas.0409402102
- Tartari, M., Gissi, C., Lo Sardo, V., Zuccato, C., Picardi, E., Pesole, G., Cattaneo, E., 2008. Phylogenetic comparison of huntingtin homologues reveals the appearance of a primitive polyQ in sea urchin. *Mol. Biol. Evol.* 25, 330–338. doi:10.1093/molbev/msm258
- The Huntington's Disease Collaborative Research Group, 1993. A novel gene containing a trinucleotide repeat that is expanded and unstable on Huntington's disease chromosomes. *Cell* 72, 971–983.
- The HD iPSC Consortium, 2012. Induced Pluripotent Stem Cells from Patients with Huntington's Disease Show CAG-Repeat-Expansion-Associated Phenotypes. *Cell Stem Cell* 11, 264–278. doi:10.1016/j.stem.2012.04.027
- Thomas, E.A., Coppola, G., Tang, B., Kuhn, A., Kim, S., Geschwind, D.H., Brown, T.B., Luthi-Carter, R., Ehrlich, M.E., 2011. In vivo cell-autonomous transcriptional abnormalities revealed in mice expressing mutant huntingtin in striatal but not cortical neurons. *Hum. Mol. Genet.* 20, 1049–1060. doi:10.1093/hmg/ddq548
- Trapnell, C., Hendrickson, D.G., Sauvageau, M., Goff, L., Rinn, J.L., Pachter, L., 2013. Differential analysis of gene regulation at transcript resolution with RNA-seq. *Nat. Biotechnol.* 31, 46–53. doi:10.1038/nbt.2450
- Trapnell, C., Pachter, L., Salzberg, S.L., 2009. TopHat: discovering splice junctions with RNA-Seq. *Bioinformatics* 25, 1105–1111. doi:10.1093/bioinformatics/btp120

- Trushina, E., Dyer, R.B., Badger, J.D., Ure, D., Eide, L., Tran, D.D., Vrieze, B.T., Legendre-Guillemain, V., McPherson, P.S., Mandavilli, B.S., Van Houten, B., Zeitlin, S., McNiven, M., Aebbersold, R., Hayden, M., Parisi, J.E., Seeberg, E., Dragatsis, I., Doyle, K., Bender, A., Chacko, C., McMurray, C.T., 2004. Mutant Huntingtin Impairs Axonal Trafficking in Mammalian Neurons In Vivo and In Vitro. *Mol. Cell. Biol.* 24, 8195–8209. doi:10.1128/MCB.24.18.8195-8209.2004
- Trushina, E., Heldebrant, M.P., Perez-Terzic, C.M., Bortolon, R., Kovtun, I.V., Badger, J.D., Terzic, A., Estévez, A., Windebank, A.J., Dyer, R.B., Yao, J., McMurray, C.T., 2003. Microtubule destabilization and nuclear entry are sequential steps leading to toxicity in Huntington's disease. *Proc. Natl. Acad. Sci. U. S. A.* 100, 12171 –12176. doi:10.1073/pnas.2034961100
- Van Raamsdonk, J.M., Pearson, J., Bailey, C.D.C., Rogers, D.A., Johnson, G.V.W., Hayden, M.R., Leavitt, B.R., 2005a. Cystamine treatment is neuroprotective in the YAC128 mouse model of Huntington disease. *J. Neurochem.* 95, 210–220. doi:10.1111/j.1471-4159.2005.03357.x
- Van Raamsdonk, J.M., Pearson, J., Murphy, Z., Hayden, M.R., Leavitt, B.R., 2006. Wild-type huntingtin ameliorates striatal neuronal atrophy but does not prevent other abnormalities in the YAC128 mouse model of Huntington disease. *BMC Neurosci.* 7, 80. doi:10.1186/1471-2202-7-80
- Van Raamsdonk, J.M., Pearson, J., Slow, E.J., Hossain, S.M., Leavitt, B.R., Hayden, M.R., 2005b. Cognitive dysfunction precedes neuropathology and motor abnormalities in the YAC128 mouse model of Huntington's disease. *J. Neurosci.* 25, 4169–4180. doi:10.1523/JNEUROSCI.0590-05.2005

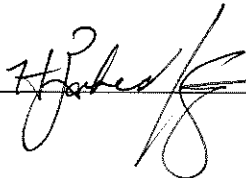
- Varma, H., Yamamoto, A., Sarantos, M.R., Hughes, R.E., Stockwell, B.R., 2010. Mutant Huntingtin Alters Cell Fate in Response to Microtubule Depolymerization via the GEF-H1-RhoA-ERK Pathway. *J. Biol. Chem.* 285, 37445–37457. doi:10.1074/jbc.M110.125542
- Verret, L., Mann, E.O., Hang, G.B., Barth, A.M.I., Cobos, I., Ho, K., Devidze, N., Masliah, E., Kreitzer, A.C., Mody, I., Mucke, L., Palop, J.J., 2012. Inhibitory interneuron deficit links altered network activity and cognitive dysfunction in Alzheimer model. *Cell* 149, 708–721. doi:10.1016/j.cell.2012.02.046
- Vöikar, V., Rauvala, H., Ikonen, E., 2002. Cognitive deficit and development of motor impairment in a mouse model of Niemann-Pick type C disease. *Behav. Brain Res.* 132, 1–10. doi:10.1016/S0166-4328(01)00380-1
- Vonsattel, J.P., DiFiglia, M., 1998. Huntington disease. *J. Neuropathol. Exp. Neurol.* 57, 369–384.
- Vossel, K.A., Zhang, K., Brodbeck, J., Daub, A.C., Sharma, P., Finkbeiner, S., Cui, B., Mucke, L., 2010. Tau Reduction Prevents A β -Induced Defects in Axonal Transport. *Science* 330, 198. doi:10.1126/science.1194653
- Walker, F.O., 2007. Huntington's disease. *Lancet* 369, 218–228. doi:10.1016/S0140-6736(07)60111-1
- Wang, Z., Gerstein, M., Snyder, M., 2009. RNA-Seq: a revolutionary tool for transcriptomics. *Nat. Rev. Genet.* 10, 57–63. doi:10.1038/nrg2484
- Wexler, N.S., 2004. Venezuelan kindreds reveal that genetic and environmental factors modulate Huntington's disease age of onset. *Proc. Natl. Acad. Sci. U. S. A.* 101, 3498–3503. doi:10.1073/pnas.0308679101

- Wyszynski, M., Kharazia, V., Shanghvi, R., Rao, A., Beggs, A.H., Craig, A.M., Weinberg, R., Sheng, M., 1998. Differential regional expression and ultrastructural localization of alpha-actinin-2, a putative NMDA receptor-anchoring protein, in rat brain. *J. Neurosci. Off. J. Soc. Neurosci.* 18, 1383–1392.
- Wyszynski, M., Lin, J., Rao, A., Nigh, E., Beggs, A.H., Craig, A.M., Sheng, M., 1997. Competitive binding of alpha-actinin and calmodulin to the NMDA receptor. *Nature* 385, 439–442. doi:10.1038/385439a0
- Zeitlin, S., Liu, J.P., Chapman, D.L., Papaioannou, V.E., Efstratiadis, A., 1995. Increased apoptosis and early embryonic lethality in mice nullizygous for the Huntington's disease gene homologue. *Nat. Genet.* 11, 155–163. doi:10.1038/ng1095-155
- Zeron, M.M., Hansson, O., Chen, N., Wellington, C.L., Leavitt, B.R., Brundin, P., Hayden, M.R., Raymond, L.A., 2002. Increased Sensitivity to N-Methyl-D-Aspartate Receptor-Mediated Excitotoxicity in a Mouse Model of Huntington's Disease. *Neuron* 33, 849–860. doi:10.1016/S0896-6273(02)00615-3
- Zhang, H., Li, Q., Graham, R.K., Slow, E., Hayden, M.R., Bezprozvanny, I., 2008. Full length mutant huntingtin is required for altered Ca²⁺ signaling and apoptosis of striatal neurons in the YAC mouse model of Huntington's disease. *Neurobiol. Dis.* 31, 80–88. doi:10.1016/j.nbd.2008.03.010

Publishing Agreement

It is the policy of the University to encourage the distribution of all theses, dissertations, and manuscripts. Copies of all UCSF theses, dissertations, and manuscripts will be routed to the library via the Graduate Division. The library will make all theses, dissertations, and manuscripts accessible to the public and will preserve these to the best of their abilities, in perpetuity.

I hereby grant permission to the Graduate Division of the University of California, San Francisco to release copies of my thesis, dissertation, or manuscript to the Campus Library to provide access and preservation, in whole or in part, in perpetuity.

Author Signature  _____ Date 04/16/18